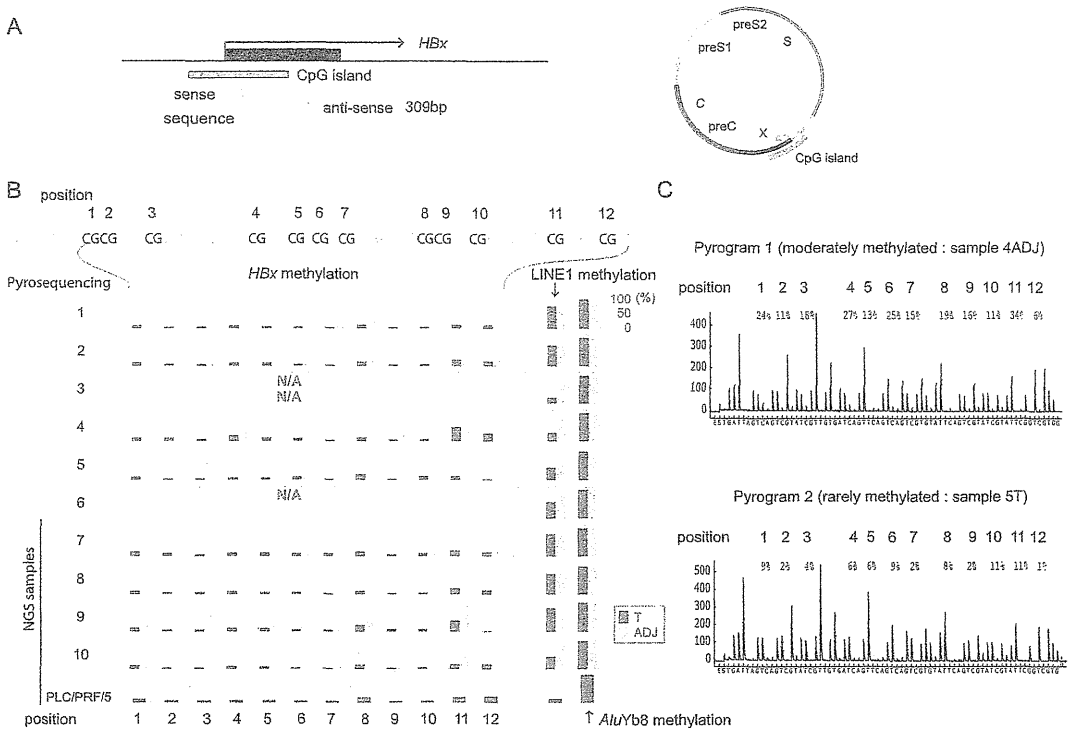

Figure 1. Methylation analysis of the CGI of the *HBx* gene. (*A*) Schema of the CGI of the *HBx* gene. Three arrows show the pyrosequencing primers used for the methylation analysis. (*B*) DNA methylation levels of the CpGs of the *HBx* gene, LINE1, and *AluYb8* in 10 paired HBV-HCC and adjacent nontumor tissue samples and PLC/PRF/5 DNA were analyzed using bisulfite pyrosequencing. Methylation levels of *HBx* varied across samples and were generally lower in HCC tissues than in the adjacent nontumor tissues. An association between *HBx* methylation levels and those of the LINE1 and *AluYb8* repeats was not observed. N/A, could not be analyzed. DNAs from four paired HBV-HCC and adjacent nontumor tissue samples (sample nos. 7–10), PLC/PRF5, and HepG2.2.15 were further analyzed using the NGS (G-NaVI method). (C) Representative pyrograms showing DNA methylation levels of the CpGs of the *HBx* gene. Methylation levels at 12 CpG sites of the *HBx* gene in adjacent nontumor tissue (sample no. 4ADJ) and tumor tissue (sample no. 5T) are shown.

DNA methylation of the integrated HBV genome as well as the adjacent human genome in cell lines

DNA methylation of the integrated HBV genome, as well as the adjacent human genome, was analyzed by bisulfite pyrosequencing. We detected varying levels of methylation of the HBV sequences integrated into the genome of PLC/PRF/5 cells (Fig. 3; Supplemental Fig. 7). Our data suggest DNA methylation in the integrated HBV genome is related to the methylation status of the integration sites within the human genome. We further characterized the methylation status of the HBV genome and human genome by allele-specific DNA methylation analysis (Fig. 3A), which revealed that the HBV genome often showed significant methylation when integrated into highly methylated sites in the human genome; however, the HBV genome remained largely unmethylated when integrated into unmethylated regions such as promoters (Fig. 3B). Integration of the HBV genome did not affect the methylation status of the human genome, including the promoter regions of the *TERT* and *SNX15* genes. Methylation of HBV DNA integrated into HepG2.2.15 cells transformed with HBV DNA (using a head-to-tail dimer) was further analyzed by bisulfite pyrosequencing, which revealed that the HBV genome generally showed significant methylation when integrated into highly methylated regions of the human genome; however, the HBV genome remains largely unmethylated when integrated into unmethylated regions (Fig. 3A).

DNA methylation levels in orthologous loci

We examined methylation levels of orthologous loci in HepG2.2.15 cells and in peripheral blood lymphocytes (PBLs) of a healthy volunteer and compared them to the methylation levels at the same (empty) target sites of PLC/PRF/5 cells. Methylation levels of orthologous loci in HepG2.2.15 cells and PBLs were generally similar to those of PLC/PRF/5 cells (Fig. 3B). Similarly, we examined methylation levels of orthologous loci in PLC/PRF/5 cells and in PBLs of a healthy volunteer and compared them to the methylation levels at the same (empty) target sites of HepG2.2.15 cells. Methylation levels of orthologous loci in PLC/PRF/5 cells and PBLs were also generally similar to those of HepG2.2.15 cells (Fig. 3B).

DNA methylation of the integrated HBV genome and the adjacent human genome in HCC tissues

To determine whether our results are relevant to human tumors, we used bisulfite pyrosequencing to investigate the methylation status of the HBV and human genomes in surgical specimen pairs of HCC and adjacent nontumor tissues. We detected no common HBV integration site (Fig. 4; Supplemental Fig. 8). Recurrent HBV integration into the *SLC6A13* gene was observed in cancerous tissues. Integration sites were rarely detected in exonic regions of the DNA from HBV-HCC samples (Fig. 4; Supplemental Fig. 8). Similar to the results obtained from the PLC/PRF/5 and HepG2.2.15 cells, our analysis revealed that the HBV genome became significantly

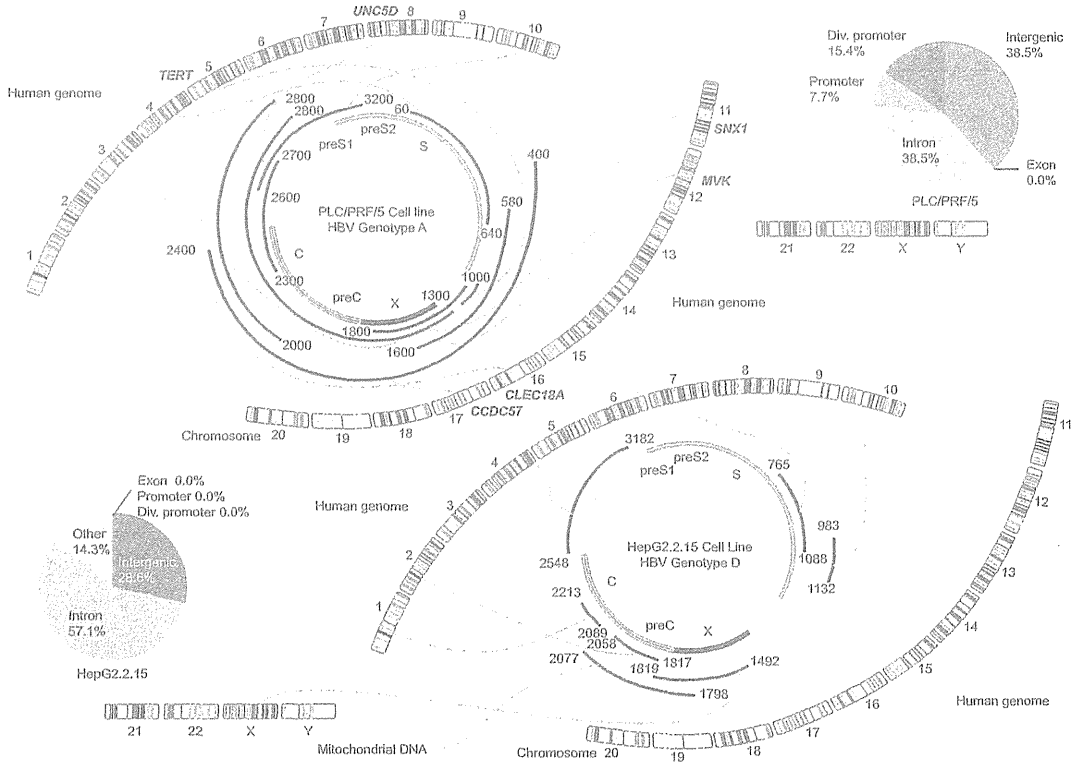

Figure 2. Distribution of the integration sites in the HBV genome and human chromosomes represented by Circos plots of the PLC/PRF/5 genome and the HepG2.2.15 genome. HBV DNA integration was analyzed using the G-NaVI method in the genome of PLC/PRF/5 cells and HepG2.2.15 cells. A common HBV integration site was not detected. Integration sites were not detected in exonic regions of the DNA from cell lines (Venn diagrams). The HBV genes (*PreC, Precore; C, Core; PreS, Presurface; S, Surface; X, X*) and the 24 human chromosomes are shown.

methylated when integrated into highly methylated human genome regions but not when integrated into unmethylated human genome regions (Fig. 4).

Correlation between the methylation pattern of the integrated HBV DNA and the human genome

DNA fragments, including 200 bp of the HBV DNA and 200 bp of the human genome around the boundary, were analyzed for average methylation, GC content, and repetitive sequences. A statistically significant correlation was observed between the average methylation of the HBV DNA and that of the human genome in cell lines and clinical samples (Fig. 5A–C; Supplemental Table 2). In contrast, average methylation did not correlate with GC content or repetitive sequences in the human and viral genome (Fig. 5D,E; Supplemental Table 2).

Using Bander software, we analyzed the chromatin structure at the integrated HBV site in PLC/PRF/5 and HepG2.2.15. Open chromatin and heterochromatin were observed more frequently at the integrated HBV in PLC/PRF/5 and HepG2.2.15, respectively (Supplemental Table 3). The difference may reflect the fact that PLC/PRF/5 is a naturally derived HBV-positive cell line and HepG2.2.15 is an HBV DNA-transfected cell line.

Discussion

We developed an NGS-based method for structural methylation analysis of integrated viral genomes. This method is a novel approach that enables the enrichment of viral fragments for sequencing using unique baits based only on the sequence of the HBV genome. We detected all regions of the human genome that harbored integrated HBV genomes without conducting unnecessary sequencing of regions where the HBV genome was not integrated. Because this technique only requires sequencing a small region of DNA around the integrated HBV sequences, a sufficient number of sequence reads can be acquired.

Methylation of viral DNA in infected cells may alter the expression patterns of viral genes related to infection and transformation (Burgers et al. 2007; Fernandez et al. 2009) and may clarify why certain infections are either cleared or persist with or without progression to precancer (Mirabello et al. 2012). To the best of our knowledge, we have, for the first time, established that the de novo patterns of DNA methylation in the integrated HBV genome are related to the methylation status of the integration sites within the human genome. A statistically significant correlation between the average methylation of the HBV DNA and that of the human genome in cell lines and clinical samples has greatly substantiated our findings. It is possible that the HBV genome becomes inactivated by methylation, when it is integrated into highly methylated host sites; therefore, HBV methylation may not contribute to tumor development. However, after integration into unmethylated human genome regions such as promoters, the HBV DNA remains unmethylated and may eventually play an important role in tumorigenesis (Fig. 6). Because multiple HBV integration sites were present in each of the analyzed samples, there remains the possibility of an asso-

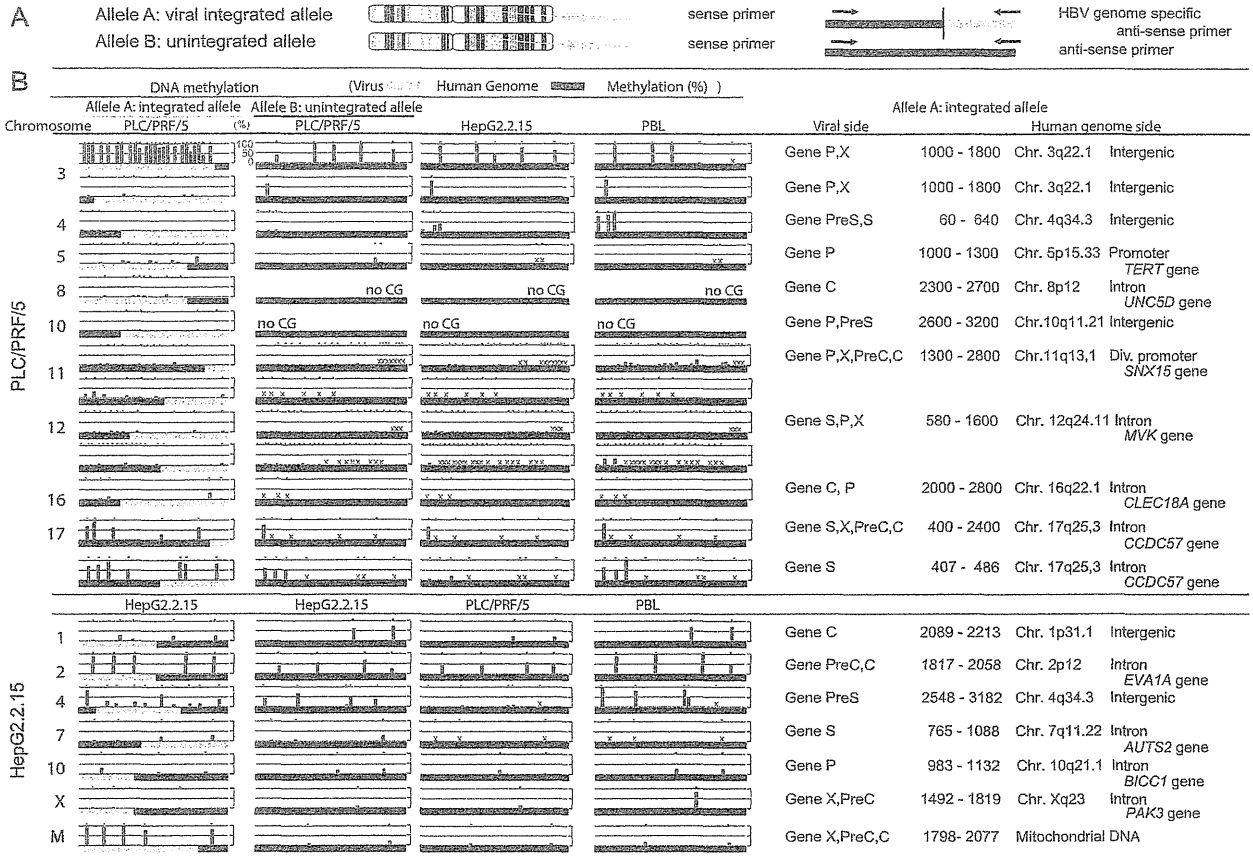

Figure 3. Allele-specific methylation analysis of the PLC/PRF/5 genome and the HepG2.2.15 genome. (*A*) A schema of allele-specific methylation analysis. (*B*) The methylation levels of the HBV and human genomes for the integrated and unintegrated alleles. Detailed results of the HBV integrants (*PreC, Precore; C, Core; PreS, Presurface; S, Surface; X, X*) and flanking host genomes (position, chromosome, location of the genome, and gene names) are shown. DNA methylation of the integrated HBV genome as well as the flanking human genome was examined by allele-specific DNA methylation analysis using bisulfite pyrosequencing. The HBV genome often showed significant methylation when integrated into highly methylated sites in the human genome; however, the HBV genome remained largely unmethylated when integrated into unmethylated regions. Methylation levels of orthologous loci in HepG2.2.15 cells and in PBLs of a healthy volunteer were examined and compared to the methylation levels at the same (empty) target sites of PLC/PRF/5 cells. Methylation levels of orthologous loci in HepG2.2.15 cells and PBLs were generally similar to those of PLC/PRF/5 cells. Similarly, methylation levels of orthologous loci in PLC/PRF/5 cells and in PBLs of a healthy volunteer were examined and compared to the methylation levels at the same (empty) target sites of HepG2.2.15 cells. Methylation levels of orthologous loci in PLC/PRF/5 cells and PBLs were generally similar to those of HepG2.2.15 cells. (×) The desired quantitative methylation levels were not obtained because of technical difficulties with the sequences that were being analyzed.

ciation between methylation and viral transcript levels. The biological impact of methylation on viral transcript levels or viral function, induced by viral insertions, also needs to be further addressed.

Methylation levels of orthologous loci in other samples at the same (empty) target sites of PLC/PRF/5 were generally similar to those of PLC/PRF/5. Similar results were observed in HepG2.2.15. These data suggest that a "before and after" relationship exists between methylation levels at preexisting target sites and those within viral insertions. At the same time, we cannot rule out the possibility that the integration of the virus subsequently affects the methylation established at the flanking target site, perhaps by acting in trans on the empty target site-containing allele. Therefore, this issue needs to be further addressed.

Differences in the integrated viral sequences could have a direct impact on the amount of cytosine methylation observed. In cases where the integration site is a highly active promoter, comparisons of methylation statuses may not be informative. Additional studies, using a large number of samples, are needed to address this issue.

Our results are notable because other studies have detected a statistically significant enrichment of HBV integration into regulatory regions, particularly promoters, in tumors (Sung et al. 2012; Toh et al. 2013); this observation may be explained by the relatively open chromatin structure of promoter regions. Average methylation did not correlate with GC content or repetitive sequences in the human and viral genomes. The relationship between methylation of HBV sequences and chromatin structure remains to be clarified because of the limitation of the Bander software used in this study. Although the mechanism needs clarification, the significant enrichment of HBV integration into regulatory regions would favor integrated HBV nonmethylation and lead to tumorigenesis. Alternatively, while the integration of HBV into the host genome may be random, HBV integration into regulatory regions is positively selected during tumorigenesis (Toh et al. 2013).

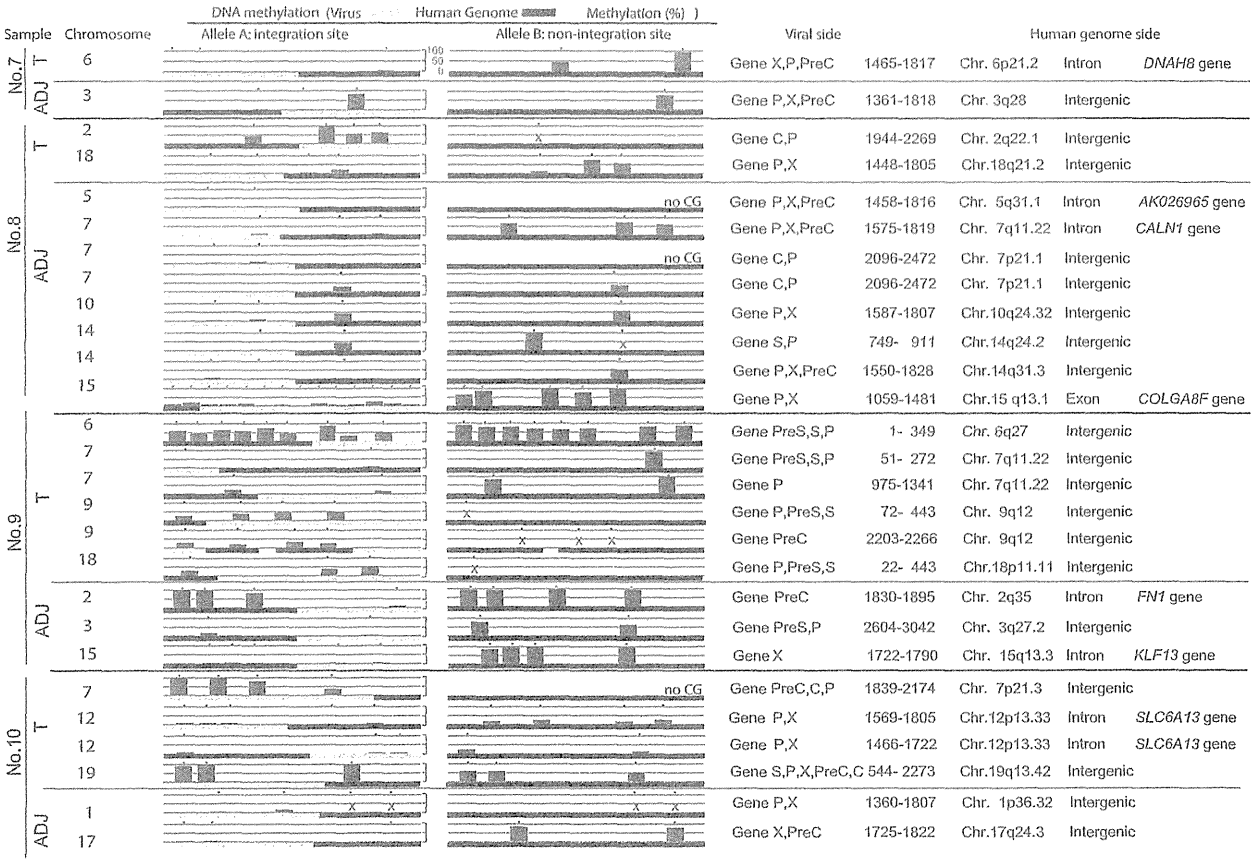

Figure 4. Allele-specific methylation analysis of the tumor (*T*) and adjacent nontumor (ADJ) sample genomes. The methylation levels of the HBV and human genomes for the integrated and unintegrated alleles in four paired tumor and adjacent nontumor samples (sample nos. 7–10) are shown. Detailed results of the HBV integrants (*PreC, Precore; C, Core; PreS, Presurface; S, Surface; X, X*) and flanking host genomes (position, chromosome, location of the genome, and gene names) are shown. The HBV genome became significantly methylated when integrated into highly methylated human genome regions, but not when integrated into unmethylated human genome regions. (×) The desired quantitative methylation levels were not obtained because of technical difficulties with the sequences that were being analyzed.

The dynamic changes in DNA methylation described here have a major functional impact on the biological behavior of HBV and underlie the molecular mechanisms that control infection or enable tumorigenesis. These findings may significantly impact public health given that millions of people worldwide are carriers of HBV. Distinct DNA methylation profiles may exist, for example, between primary HCCs in Japanese patients and those of other nationalities. Additional studies are needed to address this issue, and research into the influence of other environmental factors is required.

Increased viral DNA methylation is present in cancers associated with DNA viruses, including human papilloma virus types 16 and 18 (HPV 16 and 18) (Fernandez et al. 2009; Mirabello et al. 2012), Epstein-Barr virus (Uozaki and Fukayama 2008; Fernandez et al. 2009), and human T-lymphotropic virus 1 (Taniguchi et al. 2005). An analysis of the haplotype-resolved genome and epigenome of the aneuploid HeLa cervical cancer cell line revealed that an amplified, highly rearranged region of chromosome 8q24.21 harboring an integrated HPV18 genome likely represents the tumor-initiating event (Adey et al. 2013). Whether the dynamic changes in DNA methylation observed in cells with integrated HBV genomes also occur in human cells infected by other viruses is an interesting question for further study. We anticipate that our assay will be a powerful tool for this purpose and have successfully detected integrated HPV sequences in the genomes of cervical cancer cell lines (Y Watanabe, H Yamamoto, F Itoh, and N Suzuki, unpubl.).

This study provides novel mechanistic insights into HBV-mediated hepatocarcinogenesis, which may have preventive and therapeutic applications for carriers of HBV and patients with HBV-HCC, as it suggests that epigenetic alterations provide candidate biochemical markers and therapeutic targets. This study, together with a recent global survey of HBV integration events (Ding et al. 2012; Fujimoto et al. 2012; Jiang et al. 2012; Sung et al. 2012; Toh et al. 2013), provides a foundation for the further experimentation and mechanistic understanding of HBV-HCC.

Methods

Cell lines and primary tissues

The PLC/PRF/5 (Alexander) human hepatoma cell line was obtained from the Japanese Collection of Research Bioresources (JCRB). HepG2.2.15 cells, kindly gifted by Professor Stephan Urban

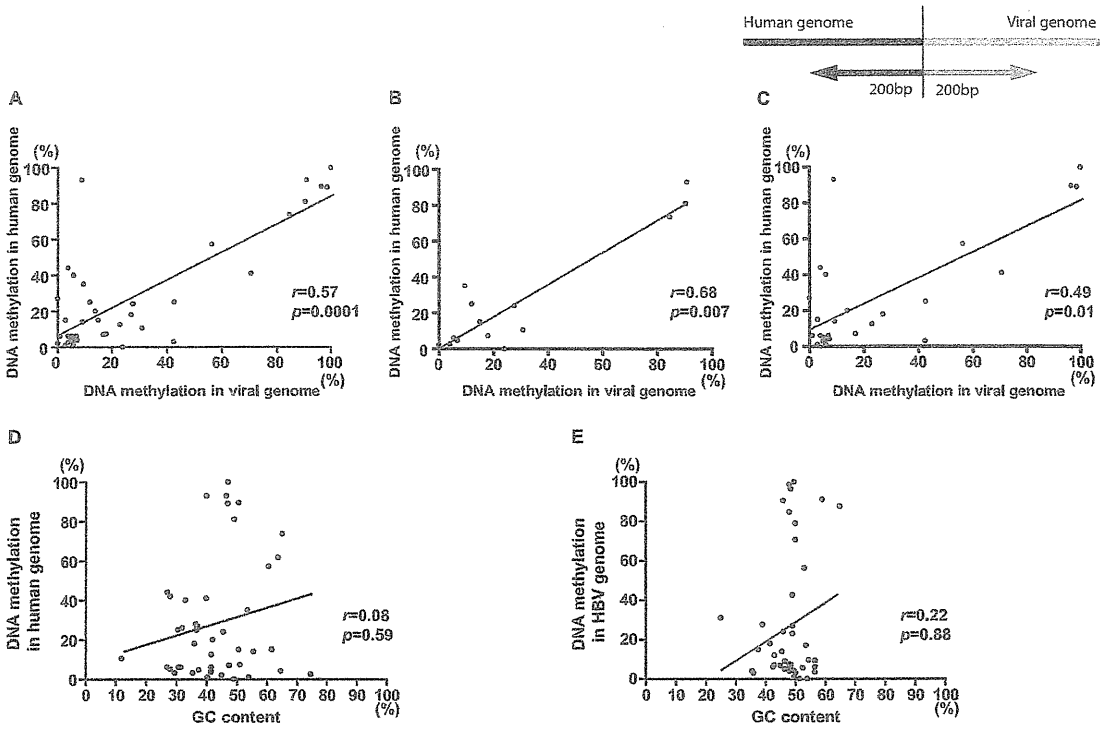

Figure 5. Correlation analysis between the methylation pattern of the integrated HBV DNA and that of the human genome. DNA fragments, including 200 bp of the HBV DNA and 200 bp of the human genome around the boundary, were analyzed for average methylation and GC content. (*A*) A correlation between the average methylation of the HBV DNA and that of the human genome in combined two cell lines and eight clinical samples ($n = 40$, $r = 0.57$, $P = 0.0001$, 95%CI = 0.3091–0.7545). (*B*) A correlation between the average methylation of the HBV DNA and that of the human genome in two cell lines ($n = 14$, $r = 068$, $P = 0.007$, 95%CI = 0.2233–0.8946). (*C*) A correlation between the average methylation of the HBV DNA and that of the human genome in eight clinical samples ($n = 26$, $r = 0.49$, $P = 0.01$, 95%CI = 0.1222–0.7463). (*D*) No correlation between the average methylation and GC contents in the human genome in the combined two cell lines and eight clinical samples ($n = 45$, $r = 0.08$, $P = 0.59$, 95%CI = −0.2253–0.3745). (*E*) No correlation between the average methylation and GC contents in the viral genome in the combined two cell lines and eight clinical samples ($n = 47$, $r = 0.22$, $P = 0.88$, 95%CI = −0.3151–0.2751).

at University Hospital Heidelberg, was derived from HepG2 cells transfected with a plasmid carrying four 5′-3′ tandem copies of the HBV genome (Koike et al. 1994). Cell lines were maintained in appropriate media containing 10% fetal bovine serum in plastic culture plates. Primary tissues from tumor and adjacent tissues were obtained at the time of the clinical procedures. Informed consent was obtained from all the patients before specimen collection. This study was approved by the institutional review board. DNA was extracted using the standard phenol–chloroform method. The concentration and quantity of extracted DNA were measured using a NanoDrop spectrophotometer (NanoDrop Technologies).

MCAM analysis

MCAM analysis was conducted as previously described (Oishi et al. 2012). A detailed protocol of MCA was previously described (Toyota et al. 1999). We used a custom human promoter array (G4426A-02212; Agilent Technologies) comprising 36,579 probes corresponding to 9021 unique genes. The probes on the array were selected to recognize SmaI/XmaI fragments mainly derived from sequences near gene transcription start sites. Five micrograms of genomic DNA was digested with 100 U of methylation-sensitive restriction endonuclease SmaI (New England Biolabs) for 24 h at 25°C, which cleaves unmethylated DNA leaving blunt ends (CCC/GGG). Subsequently, the DNA was digested with 20 U of methylation-insensitive restriction endonuclease XmaI for 6 h at 37°C, creating sticky ends (C/CCGGG). Five hundred milligrams of digested DNA was ligated using 50 μL of RMCA12 (5′-CCGGGCA GAAAG-3′)/RMCA24 (5′-CCACCGCCATCCGAGCCTTTCTGC-3′) primers and T4 DNA ligase (TaKaRa Bio) for 16 h at 16°C. After filling in the overhanging ends of the ligated DNA fragments at 72°C, the DNA was amplified for 5 min at 95°C followed by 25 cycles of 1-min incubation at 95°C and 3-min incubation at 77°C using 100 pmol of RMCA24 primer. MCA products were labeled with Cy5 (red) for DNA from hepatoma samples (both tumor and adjacent normal) and Cy3 (green) for DNA from human blood mixture of three healthy volunteers using a randomly primed Klenow polymerase reaction (Invitrogen) for 3 h at 37°C. Human CpG island arrays (4 × 44 K) were purchased from Agilent Technologies. Microarray protocols, including labeling, hybridization, and post-hybridization washing procedures, are provided at http://www.agilent.com/. Labeled samples were then hybridized to arrays in the presence of human Cot-1 DNA for 24 h at 65°C. After washing, arrays were scanned using an Agilent DNA microarray scanner and analyzed using Agilent Feature Extraction software (FE version 9.5.1.1, Agilent Technologies) at St. Marianna University School of Medicine. We used GeneSpring software (Agilent) for choosing candidate genes after normalization of the raw data.

DNA methylation analysis

Hidden Markov models have been successfully used to partition genomes into segments of comparable stochastic structure (Durbin et al. 1998). Using these models for sequence analysis performed

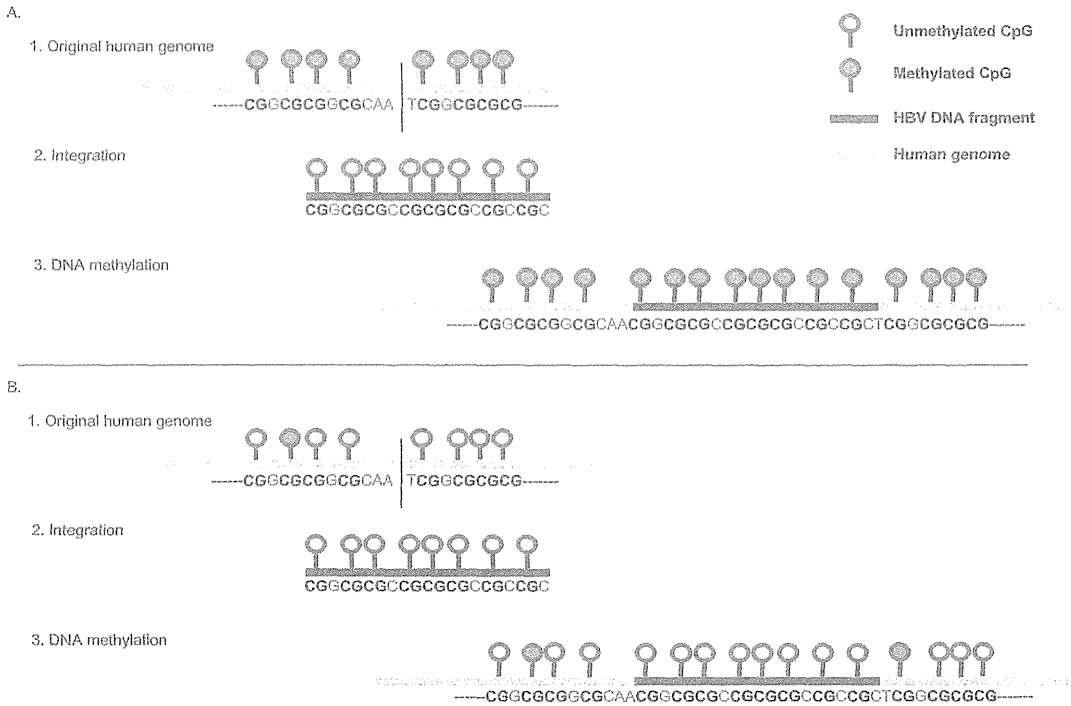

Figure 6. Schema of DNA methylation at HBV integrants and flanking human genomic sequences. (*A*) DNA hypermethylation was seen in both the integrated HBV fragment and human genome (original human genome shows dense methylation). The HBV genome often showed significant methylation when integrated into highly methylated host sites. (*B*) DNA hypermethylation was rarely seen in the integrated HBV fragment and human genome (original human genome shows low methylation). The HBV genome remained largely unmethylated when integrated into unmethylated host sites.

on the CpG plugin of bioinformatics software Geneious 5.5.8 (Biomatters), CpG islands were searched in the HBV genome (Kearse et al. 2012). Bisulfite PCR was performed using an EpiTect Bisulfite Kit (Qiagen) according to the manufacturer's protocol. One microliter of bisulfite-treated DNA was used as a template. The primers used for amplifying CpG sequences in the *HBx* gene are described in Supplemental Table 1. After PCR, the biotinylated strand was captured on streptavidin-coated beads (Amersham Bioscience) and incubated with sequencing primers (Supplemental Table 1). The pyrosequencing reactions were performed using the PyroMark Q24 and/or PyroMark Q24 advanced (Qiagen). Pyrosequencing quantitatively measures the methylation status of several CpG sites in a given sequence. These adjacent sites usually show highly concordant methylation. Therefore, the mean percentage of methylation at detected sites was used as a representative value for each sequence.

LINE1 and *Alu*Yb8 methylation analysis

The LINE1 and *Alu*Yb8 methylation levels, as measured by pyrosequencing, are good indicators of the cellular levels of 5-methylcytosine (i.e., the global DNA methylation level). To quantify relatively high LINE1 and *Alu*Yb8 methylation levels, we used pyrosequencing technology (Igarashi et al. 2010). PCR and subsequent pyrosequencing for LINE1 and *Alu*Yb8 were performed using the PyroMark kit (Qiagen). This assay amplifies a region of the LINE1 or *Alu*Yb8 elements that includes three CpG sites. The PCR was conducted as follows: 45 cycles for 20 sec at 95°C, for 20 sec at 50°C, and for 20 sec at 72°C, followed by 5 min at 72°C. The biotinylated PCR product was purified and converted to single strands to serve as a template for the pyrosequencing reaction using the pyrosequencing vacuum prep tool (Qiagen). The pyrosequencing reactions were performed using the PyroMark Q24 and/or PyroMark Q24 advanced (Qiagen). The percentage of Cs relative to the total sum of the Cs and Ts at each CpG site was calculated. The average of the percentages of Cs at the three CpG sites was used to represent the overall LINE1 and *Alu*Yb8 methylation levels in each sample.

FISH analysis of HBV integration

We developed a FISH analysis method to detect HBV DNA and demonstrate its presence in PLC/PRF/5 cells (Supplemental Fig. 3). The slides were pretreated with hydrogen peroxide and rinsed in 1× phosphate-buffered saline (PBS) to minimize background and quench endogenous peroxidase activity. To remove the excess cytoplasm, the slides were treated with pepsin and then fixed with 1% formaldehyde in PBS/$MgCl_2$. The slides were then dehydrated in an ethanol series (70%, 90%, and 100%) for 3 min at each step. The probes were designed based on the reference HBV sequence in PLC/PRF/5 DNA that is available from the Methylyzer 1.0 website (http://gbrowse.bioinfo.cnio.es/cgi-bin/VIRUS/HBV/). The FISH probes were prepared by combining the PCR-labeled probes (Supplemental Table 1), human Cot-1 DNA, and salmon sperm DNA. The probes were precipitated and mixed with hybridization buffer, and the probe DNA cocktail was denatured for 5 min at 95°C. The DNA on the slides was denatured by soaking in 70% formamide/2× SSC for 3 min at 74°C. The slides were immediately immersed in freshly prepared ice-cold 70% ethanol for 3 min, followed by 3-min immersions in 90% and then 100% ethanol. The denatured probe DNA was applied to the dry denatured slides and covered with a coverslip. The hybridization was performed for 16 h at 37°C.

Tyramide signal amplification (TSA)–FISH

TSA (tyramide signal amplification) detection kits were obtained from PerkinElmer. TSA-FISH detection was performed following the manufacturer's protocols with minor modifications. High stringency washes (0.1× SSC) were used to reduce the background, and TNT buffer (0.1 M Tris-HCl at pH 7.5, 0.15 M NaCl, 0.05% Tween 20) was adjusted to pH 7.0–7.5. The biotin- or DIG-labeled probes were detected using streptavidin-HRP or anti-DIG-HRP in TNB (0.1 M Tris-HCl at pH 7.5, 0.15 M NaCl, 0.05% blocking reagent [supplied in the kit]) for 30 min at room temperature and washed twice for 5 min each in TNT buffer. For the tyramide amplification procedure, the slide was covered with tyramide solution (Tyr-Bio, 1:50) for 10 min at room temperature. The tyramide solution was removed, and the slides were washed twice for 5 min each with TNT at room temperature. Fluorochrome-conjugated streptavidin (stAv-Alexa 488) diluted in TNB was used to detect the Tyr-Bio. The slides were incubated for 30 min at room temperature, washed with TNT buffer twice for 5 min each at room temperature, and covered with an anti-fade reagent containing DAPI (Speel et al. 1997; Schriml et al. 1999).

Identification of the chromosomal locations of viral–host junctions

The viral–host junctions were amplified using primers specific for human *Alu*Yb8 repetitive sequences and HBV X regions (Supplemental Table 1; Minami et al. 1995; Murakami et al. 2004). One microliter of genomic DNA solution served as a template in the subsequent PCR. We used touchdown PCR for most of the assays. All PCR assays included a denaturation step for 30 sec at 95°C, followed by an annealing step at various temperatures for 30 sec and an extension step for 30 sec at 72°C. PCR products were analyzed using electrophoresis through 1% agarose gels. PCR products were ligated to pCR-XL-TOPO vector DNA (TOPO XL PCR Cloning kit; Invitrogen) and transformed into competent cells. Positive colonies were selected and isolated using a QIA prep Spin Miniprep Kit (Qiagen). Direct sequence analysis of TOPO-TA cloning products was performed using a 3130 genetic analyzer (Applied Biosystems) (Watanabe et al. 2011). All sequences were searched for matches with HBV and pCR-XL-TOPO sequences using Geneious 5.5.8 (Biomatters) sequence analysis and assembly software and the BLAST program available on the UCSC Genome Browser (http://genome.ucsc.edu/).

Analysis of HBV DNA integration site sequences using NGS

Agilent's SureSelect target enrichment system is a highly efficient hybrid selection technique for optimizing NGS. We used this system and 12,391 custom baits covering the DNA sequences of HBV genotypes A to J and PLC/PRF/5 HBV sequences and optimized experiments for a GS FLX Titanium system (Roche). PLC/PRF/5, HepG2.2.15, and four paired tumor and nontumor samples (sample nos. 7, 8, 9, and 10 in Fig. 1B) were analyzed.

DNA methylation analysis of the integrated HBV genome as well as the adjacent human genome

DNA methylation was analyzed using bisulfite pyrosequencing (Oishi et al. 2012). The pyrosequencing reactions were performed using the PyroMark Q24 and/or PyroMark Q24 advanced (Qiagen). PLC/PRF/5, HepG2.2.15, and four paired tumor and nontumor samples (sample nos. 7, 8, 9, and 10 in Fig. 1B) were analyzed. Primers for methylation analysis of integration sites in PLC/PRF/5 are shown in Supplemental Table 1.

DNA methylation analysis of orthologous loci

Methylation levels of orthologous loci in HepG2.2.15 cells and in PBLs of a healthy volunteer at the same (empty) target sites of PLC/PRF/5 cells were analyzed using bisulfite pyrosequencing. Similarly, methylation levels of orthologous loci in PLC/PRF/5 cells and in PBLs at the same (empty) target sites of HepG2.2.15 cells were analyzed.

Allele-specific DNA methylation analysis of the integrated HBV genome as well as the adjacent human genome

Allele-specific DNA methylation was analyzed as described previously (Yamada and Ito 2011). The pyrosequencing reactions were performed using the PyroMark Q24 and/or PyroMark Q24 advanced (Qiagen).

Correlation analysis between the methylation pattern of the integrated HBV DNA and that of the human genome

DNA fragments, including 200 bp of the integrated HBV DNA and 200 bp of the human genome around the boundary, were analyzed for average methylation, GC content, and repetitive sequences in cell lines and clinical samples. RepeatMasker was used to identify repetitive elements in genomic sequences (AFA Smit, R Hubley, P Green, unpubl.). The Spearman correlation coefficient was used to assess correlations between the average methylation of the HBV DNA and that of the human genome. Correlations between GC content or repetitive sequences in the HBV DNA and the human genome were analyzed by using the Spearman correlation coefficient for continuous variables, and $P < 0.05$ was considered significant. All statistical analyses were performed using PRISM software for Windows, version 4 (GraphPad Prism).

Chromatin structure at the integrated HBV site

Using Bander software (Cheung et al. 2001; Furey and Haussler 2003), we analyzed the chromatin structure at the integrated HBV site in PLC/PRF/5 and HepG2.2.15.

Data access

All raw sequence data from this study have been submitted to the DDBJ Japanese Genotype-phenotype Archive (JGA; http://trace.ddbj.nig.ac.jp/jga/index_e.html) under accession number JGAS00000000015. Array data have been submitted to the NCBI Gene Expression Omnibus (GEO; http://www.ncbi.nlm.nih.gov/geo/) under accession number GSE59405.

Acknowledgments

We thank Drs. K. Watashi and T. Wakita for cell lines and Drs. T. Takayama, K. Takasaki, and S. Kawasaki for clinical samples. We also thank Drs. N. Matsumoto and N. Yamada-Ohkawa, as well as other members of the laboratory, for advice and suggestions. A part of the data used for this research was originally obtained by a research project of Hiroyuki Yamamoto and Yoshiyuki Watanabe led by Professor Fumio Itoh and is available at the website of the NBDC/JST (http://biosciencedbc.jp/en/). This work was supported in part by the Japan Society for the Promotion of Science (JSPS) Grants-in-Aid for Scientific Research (JSPS KAKENHI grant no. 23590964 to H. Yotsuyanagi).

Author contributions: Y.W. conceived the study, designed and performed the experiments, analyzed the data, and wrote the manuscript. H. Yamamoto designed the experiments, analyzed the data and wrote the manuscript. R.O. performed the experiments

and analyzed the data. M.T. provided intellectual support. M.Y., N.K., S.T., and A.S. provided clinical samples. H. Yotsuyanagi designed the experiments, analyzed the data and wrote the manuscript. K.K. provided intellectual support. F.I. supervised all aspects of the study.

References

Adey A, Burton JN, Kitzman JO, Hiatt JB, Lewis AP, Martin BK, Qiu R, Lee C, Shendure J. 2013. The haplotype-resolved genome and epigenome of the aneuploid HeLa cancer cell line. *Nature* **500:** 207–211.

Burgers WA, Blanchon L, Pradhan S, de Launoit Y, Kouzarides T, Fuks F. 2007. Viral oncoproteins target the DNA methyltransferases. *Oncogene* **26:** 1650–1655.

Cheung VG, Nowak N, Jang W, Kirsch IR, Zhao S, Chen XN, Furey TS, Kim UJ, Kuo WL, Olivier M, et al. 2001. Integration of cytogenetic landmarks into the draft sequence of the human genome. *Nature* **409:** 953–958.

Ding D, Lou X, Hua D, Yu W, Li L, Wang J, Gao F, Zhao N, Ren G, Li L, et al. 2012. Recurrent targeted genes of hepatitis B virus in the liver cancer genomes identified by a next-generation sequencing-based approach. *PLoS Genet* **8:** e1003065.

Doerfler W. 2008. In pursuit of the first recognized epigenetic signal-DNA methylation: a 1976 to 2008 synopsis. *Epigenetics* **3:** 125–133.

Doerfler W, Remus R, Müller K, Heller H, Hohlweg U, Schubbert R. 2001. The fate of foreign DNA in mammalian cells and organisms. *Dev Biol* **106:** 89–97.

Durbin R, Eddy S, Krogh A, Mitchison G. 1998. *Biological sequence analysis*. Cambridge University Press, Cambridge, UK.

Fernandez AF, Rosales C, Lopez-Nieva P, Graña O, Ballestar E, Ropero S, Espada J, Melo SA, Lujambio A, Fraga MF, et al. 2009. The dynamic DNA methylomes of double-stranded DNA viruses associated with human cancer. *Genome Res* **19:** 438–451.

Fujimoto A, Totoki Y, Abe T, Boroevich KA, Hosoda F, Nguyen HH, Aoki M, Hosono N, Kubo M, Miya F, et al. 2012. Whole-genome sequencing of liver cancers identifies etiological influences on mutation patterns and recurrent mutations in chromatin regulators. *Nat Genet* **44:** 760–764.

Furey TS, Haussler D. 2003. Integration of the cytogenetic map with the draft human genome sequence. *Hum Mol Genet* **12:** 1037–1044.

Gatza ML, Chandhasin C, Ducu RI, Marriott SJ. 2005. Impact of transforming viruses on cellular mutagenesis, genome stability, and cellular transformation. *Environ Mol Mutagen* **45:** 304–325.

Hilleman MR. 2004. Strategies and mechanisms for host and pathogen survival in acute and persistent viral infections. *Proc Natl Acad Sci* **101:** 14560–14566.

Igarashi S, Suzuki H, Niinuma T, Shimizu H, Nojima M, Iwaki H, Nobuoka T, Nishida T, Miyazaki Y, Takamaru H, et al. 2010. A novel correlation between LINE-1 hypomethylation and the malignancy of gastrointestinal stromal tumors. *Clin Cancer Res* **16:** 5114–5123.

Jiang Z, Jhunjhunwala S, Liu J, Haverty PM, Kennemer MI, Guan Y, Lee W, Carnevali P, Stinson J, Johnson S, et al. 2012. The effects of hepatitis B virus integration into the genomes of hepatocellular carcinoma patients. *Genome Res* **22:** 593–601.

Kan Z, Zheng H, Liu X, Li S, Barber TD, Gong Z, Gao H, Hao K, Willard MD, Xu J, et al. 2013. Whole-genome sequencing identifies recurrent mutations in hepatocellular carcinoma. *Genome Res* **23:** 1422–1433.

Kearse M, Moir R, Wilson A, Stones-Havas S, Cheung M, Sturrock S, Buxton S, Cooper A, Markowitz S, Duran C, et al. 2012. Geneious Basic: an integrated and extendable desktop software platform for the organization and analysis of sequence data. *Bioinformatics* **28:** 1647–1649.

Kim CM, Koike K, Saito I, Miyamura T, Jay DG. 1991. HBx gene of hepatitis B virus induces liver cancer in transgenic mice. *Nature* **351:** 317–320.

Koike K, Moriya K, Iino S, Yotsuyanagi H, Endo Y, Miyamura T, Kurokawa K. 1994. High-level expression of hepatitis B virus HBx gene and hepatocarcinogenesis in transgenic mice. *Hepatology* **19:** 810–819.

Lau C-C, Sun T, Ching AK, He M, Li JW, Wong AM, Co NN, Chan AW, Li PS, Lung RW, et al. 2014. Viral-human chimeric transcript predisposes risk to liver cancer development and progression. *Cancer Cell* **25:** 335–349.

Li S, Mao M. 2013. Next generation sequencing reveals genetic landscape of hepatocellular carcinomas. *Cancer Lett* **340:** 247–253.

Lupberger J, Hildt E. 2007. Hepatitis B virus–induced oncogenesis. *World J Gastroenterol* **13:** 74–81.

Minami M, Poussin K, Brechot C, Paterlini P. 1995. A novel PCR technique using *Alu*-specific primers to identify unknown flanking sequences from the human genome. *Genomics* **29:** 403–408.

Mirabello L, Sun C, Ghosh A, Rodriguez AC, Schiffman M, Wentzensen N, Hildesheim A, Herrero R, Wacholder S, Lorincz A, et al. 2012. Methylation of human papillomavirus type 16 genome and risk of cervical precancer in a Costa Rican population. *J Natl Cancer Inst* **104:** 556–565.

Murakami Y, Minami M, Daimon Y, Okanoue T. 2004. Hepatitis B virus DNA in liver, serum, and peripheral blood mononuclear cells after the clearance of serum hepatitis B virus surface antigen. *J Med Virol* **72:** 203–214.

Nakagawa H, Shibata T. 2013. Comprehensive genome sequencing of the liver cancer genome. *Cancer Lett* **340:** 234–240.

Oishi Y, Watanabe Y, Yoshida Y, Sato Y, Hiraishi T, Oikawa R, Maehata T, Suzuki H, Toyota M, Niwa H, et al. 2012. Hypermethylation of Sox17 gene is useful as a molecular diagnostic application in early gastric cancer. *Tumour Biol* **33:** 383–393.

Orend G, Kuhlmann I, Doerfler W. 1991. Spreading of DNA methylation across integrated foreign (adenovirus type 12) genomes in mammalian cells. *J Virol* **65:** 4301–4308.

Schriml LM, Padilla-Nash HM, Coleman A, Moen P, Nash WG, Menninger J, Jones G, Ried T, Dean M. 1999. Tyramide signal amplification (TSA)-FISH applied to mapping PCR-labeled probes less than 1 kb in size. *Biotechniques* **27:** 608–613.

Sells MA, Chen ML, Acs G. 1987. Production of hepatitis B virus particles in Hep G2 cells transfected with cloned hepatitis B virus DNA. *Proc Natl Acad Sci* **84:** 1005–1009.

Speel EJ, Ramaekers FC, Hopman AH. 1997. Sensitive multicolor fluorescence in situ hybridization using catalyzed reporter deposition (CARD) amplification. *J Histochem Cytochem* **45:** 1439–1446.

Sung WK, Zheng H, Li S, Chen R, Liu X, Li Y, Lee NP, Lee WH, Ariyaratne PN, Tennakoon C, et al. 2012. Genome-wide survey of recurrent HBV integration in hepatocellular carcinoma. *Nat Genet* **44:** 765–769.

Taniguchi Y, Nosaka K, Yasunaga J, Maeda M, Mueller N, Okayama A, Matsuoka M. 2005. Silencing of human T-cell leukemia virus type I gene transcription by epigenetic mechanisms. *Retrovirology* **2:** 64.

Tao Q, Robertson KD. 2003. Stealth technology: how Epstein-Barr virus utilizes DNA methylation to cloak itself from immune detection. *Clin Immunol* **109:** 53–63.

Toh ST, Jin Y, Liu L, Wang J, Babrzadeh F, Gharizadeh B, Ronaghi M, Toh HC, Chow PK, Chung AY, et al. 2013. Deep sequencing of the hepatitis B virus in hepatocellular carcinoma patients reveals enriched integration events, structural alterations and sequence variations. *Carcinogenesis* **34:** 787–798.

Toyota M, Ho C, Ahuja N, Jair KW, Li Q, Ohe-Toyota M, Baylin SB, Issa JP. 1999. Identification of differentially methylated sequences in colorectal cancer by methylated CpG island amplification. *Cancer Res* **59:** 2307–2312.

Uozaki H, Fukayama M. 2008. Epstein-Barr virus and gastric carcinoma-viral carcinogenesis through epigenetic mechanisms. *Int J Clin Exp Pathol* **1:** 198–216.

Watanabe Y, Castoro RJ, Kim HS, North B, Oikawa R, Hiraishi T, Ahmed SS, Chung W, Cho MY, Toyota M, et al. 2011. Frequent alteration of MLL3 frameshift mutations in microsatellite deficient colorectal cancer. *PLoS ONE* **6:** e23320.

Yamada Y, Ito T. 2011. Highly efficient PCR assay to discriminate allelic DNA methylation status using whole genome amplification. *BMC Res Notes* **4:** 179.

Received March 8, 2014; accepted in revised form December 29, 2014.

World Journal of Gastroenterology

Online Submissions: http://www.wjgnet.com/esps/
bpgoffice@wjgnet.com
doi:10.3748/wjg.v20.i11.3044

World J Gastroenterol 2014 March 21; 20(11): 3044-3049
ISSN 1007-9327 (print) ISSN 2219-2840 (online)

Acute hepatitis B of genotype H resulting in persistent infection

Norie Yamada, Ryuta Shigefuku, Ryuichi Sugiyama, Minoru Kobayashi, Hiroki Ikeda, Hideaki Takahashi, Chiaki Okuse, Michihiro Suzuki, Fumio Itoh, Hiroshi Yotsuyanagi, Kiyomi Yasuda, Kyoji Moriya, Kazuhiko Koike, Takaji Wakita, Takanobu Kato

Norie Yamada, Ryuichi Sugiyama, Takaji Wakita, Takanobu Kato, Department of Virology II, National Institute of Infectious Diseases, Shinjyuku-Ku, Tokyo 162-8640, Japan
Norie Yamada, Minoru Kobayashi, Kiyomi Yasuda, Department of Internal Medicine, Center for Liver Diseases, Kiyokawa Hospital, Suginami, Tokyo 166-0004, Japan
Norie Yamada, Ryuta Shigefuku, Minoru Kobayashi, Hiroki Ikeda, Hideaki Takahashi, Chiaki Okuse, Michihiro Suzuki, Fumio Itoh, Division of Gastroenterology and Hepatology, Department of Internal Medicine, St. Marianna University School of Medicine, Kanagawa 216-8511, Japan
Hiroshi Yotsuyanagi, Department of Infectious Diseases, Graduate School of Medicine, The University of Tokyo, Tokyo 113-8655, Japan
Kyoji Moriya, Department of Infection Control and Prevention, Graduate School of Medicine, The University of Tokyo, Tokyo 113-8655, Japan
Kazuhiko Koike, Department of Gastroenterology, Graduate School of Medicine, The University of Tokyo, Tokyo 113-8655, Japan
Author contributions: Shigefuku R, Kobayashi M, Ikeda H, Takahashi H, Okuse C, Suzuki M and Itoh F were the patient's attending physicians; Yotsuyanagi H, Yasuda K, Moriya K, Koike K, Wakita T and Kato T organized the study; Yamada N, Sugiyama R and Kato T performed the research; Yamada N and Kato T wrote the manuscript.
Supported by Japan Society for the Promotion of Science and the Ministry of Health, Labour and Welfare and the Ministry of Education, Culture, Sports, Science and Technology of Japan
Correspondence to: Takanobu Kato, MD, PhD, Department of Virology II, National Institute of Infectious Diseases, Toyama 1-23-1, Shinjyuku-Ku, Tokyo 162-8640, Japan. takato@nih.go.jp
Telephone: +81-3-52851111 Fax: +81-3-52851161
Received: October 3, 2013 Revised: November 18, 2013
Accepted: December 5, 2013
Published online: March 21, 2014

Abstract

A 47-year-old man presented with general fatigue and dark urine. The laboratory data showed increased levels of hepatic transaminases. The patient was positive for hepatitis B virus (HBV) markers and negative for anti-human immunodeficiency virus. The HBV-DNA titer was set to 7.7 log copies/mL. The patient was diagnosed with acute hepatitis B. The HBV infection route was obscure. The serum levels of hepatic transaminases decreased to normal ranges without any treatment, but the HBV-DNA status was maintained for at least 26 mo, indicating the presence of persistent infection. We isolated HBV from the acute-phase serum and determined the genome sequence. A phylogenetic analysis revealed that the isolated HBV was genotype H. In this patient, the elevated peak level of HBV-DNA and the risk alleles at human genome single nucleotide polymorphisms s3077 and rs9277535 in the human leukocyte antigen-DP locus were considered to be risk factors for chronic infection. This case suggests that there is a risk of persistent infection by HBV genotype H following acute hepatitis; further cases of HBV genotype H infection must be identified and characterized. Thus, the complete determination of the HBV genotype may be essential during routine clinical care of acute hepatitis B outpatients.

Key words: Acute hepatitis; Chronic hepatitis; Genotyping; Hepatitis B virus; Single nucleotide polymorphisms

Core tip: Hepatitis B virus (HBV) genotype H infection is rare in Asia, particularly in Japan. Here, we report a case of acute hepatitis B caused by a genotype H strain with persistent infection, although most adult cases of acute hepatitis B are self-limiting in Japan. This case suggests that the HBV genotype H infection can be a risk factor for persistent infection. Therefore, it is necessary to investigate the characteristics of genotype H infection in an accumulation of cases. Thus, the

complete determination of the HBV genotype may be essential in the routine clinical care of acute hepatitis B patients.

Yamada N, Shigefuku R, Sugiyama R, Kobayashi M, Ikeda H, Takahashi H, Okuse C, Suzuki M, Itoh F, Yotsuyanagi H, Yasuda K, Moriya K, Koike K, Wakita T, Kato T. Acute hepatitis B of genotype H resulting in persistent infection. *World J Gastroenterol* 2014; 20(11): 3044-3049 Available from: URL: http://www.wjgnet.com/1007-9327/full/v20/i11/3044.htm DOI: http://dx.doi.org/10.3748/wjg.v20.i11.3044

INTRODUCTION

Hepatitis B is a potentially life-threatening liver infection caused by the hepatitis B virus (HBV); it represents a major global health problem. HBV can cause chronic liver diseases and increases the risk of death from cirrhosis and liver cancer. Worldwide, an estimated two billion people have been infected with HBV and more than 240 million have chronic infections[1]. The HBV genome consists of approximately 3200-nucleotides of DNA; the virus replicates using a reverse transcriptase enzyme that lacks proofreading ability. Therefore, HBV possesses diverse genetic variability, and the viral population is classified into at least eight genotypes that are designated A -H[2-6]. In Japan, genotypes B and C are prevalent among patients with chronic infections. However, in the last decades, the prevalent genotype in acute HBV infections has shifted from genotype C to A[7-9]. There are some differences in the clinical features and outcomes among the genotypes[10-13]. It has been reported that the persistent infection from acute hepatitis is prevalent in adults that are infected with genotype A HBV. Thus, determining the HBV genotype is of increasing importance even in routine clinical practice, although a reliable kit for determination of all HBV genotypes is still uncommon and is not yet covered by insurance. The host factors associated with persistent infection by HBV have also been reported, such as single nucleotide polymorphisms (SNPs) or genotypes in the human leukocyte antigen-DP locus. It may also be useful for identifying the patients who are prone to develop chronic hepatitis.

In this report, we describe a case of acute hepatitis B resulting from infection by a genotype H strain of HBV. Although the laboratory data and symptoms were not distinguishable from acute hepatitis B with other genotypes, this patient developed persistent infection.

CASE REPORT

A 47-year-old man living in Kawasaki, Japan, presented at our hospital with general fatigue and dark urine. Approximately 1 wk before visiting the hospital, the patient developed nausea, loss of appetite, and a feeling of fullness in the abdomen. Four days later, he noted darkening of his skin and urine. Upon admission, the patient's laboratory data revealed elevated serum aspartate aminotransferase, alanine aminotransferase (ALT), lactate dehydrogenase, alkaline phosphatase, γ-glutamylt ranspeptidase, and total bilirubin (T-Bil) levels (Table 1). The prothrombin activity was within the normal range (95%). Test for hepatitis B surface antigen (HBsAg; HISCL-2000i, Sysmex, Kobe, Hyogo, Japan), hepatitis B e-antigen (HBeAg; ARCHITECT® CLIA, Abbott Japan, Tokyo, Japan) and anti-hepatitis B core antigen (anti-HBc) IgM (ARCHITECT® CLIA) were positive. A test for HBV-DNA was also positive, exhibiting a titer of 7.7 log copies/mL (COBAS TaqMan HBV Test v2.0, Roche Diagnostics, Tokyo, Japan). HBsAg had not been detected 2 years previously when the patient had been admitted to another hospital for treatment of acute enterocolitis. Other hepatitis virus markers were negative. Therefore, the patient was diagnosed with acute hepatitis B. The genotype of the infecting HBV, as assessed by the Immunis HBV Genotype Immunis® HBV Genotype EIA Kit (Institute of Immunology, Tokyo, Japan), was determined as genotype C. The patient had not been abroad in the past 12 mo; he had no history of receiving blood or blood-related products, transfusions, or drug injections, and he reported no personal or family history of liver disease. The man was unmarried and declared that he was heterosexual, with no history of sexual contact with commercial sex workers or strangers. Anti-human immunodeficiency virus (HIV) was not detected. In the absence of medication, the patient's condition and elevated ALT level improved within a month. Anti-HBe became detectable, and HBeAg disappeared 2 mo after onset of the symptoms. HBsAg became undetectable at 5 mo, but the patient still tested positive for HBV-DNA, a status that persisted for at least 26 mo following his presentation at our hospital (Figure 1). We are now preparing to administer anti-viral medication.

For further analysis of the HBV infecting this patient, HBV-DNA was extracted from the acute-phase serum using a QIAamp DNA Blood Mini kit (QIAGEN, Valencia, CA). The entire HBV genome sequence was determined after polymerase chain reaction (PCR) amplification using the following primers [the number of nucleotides (nt) added to the primers were deduced from the prototype HBV/C clone, with accession no. AB246344]. For the amplification of half of the HBV genome, the outer primers were 5'-ATTCCACCAAGCTCTGCTAGATCCCAGAGT-3' (nt 10-39) and 5'-GGTGCTGGTGAACAGACCAATTTATGCCTA-3' (nt 1813-1784), and the inner primers were 5'-CCTATATTTTCCTGCTGGTGGCTCCAGTTC-3' (nt 46-75) and 5'-TAGCCTAATCTCCTCCC CCAACTCCTCCCA-3' (nt 1760-1731). For the other half of the HBV genome, the outer primers were 5'- ACGTCGCATGGAGACCACCGTGAACGCCCA-3' (nt 1601-1630) and 5'-AAGTCCACCACGAGTCTAGACTCTGTGGTA-3' (nt 266-237), and the inner primers were 5'-CCAGGTCTTGCCCAAGGTCTTACATAAGAG-3' (nt 1631-1660) and 5'-CCCGCCTGTAACACGAGCAGGGGTCCTAGG-3' (nt 207-178). The PCR was performed in a thermal cycler for 30 cycles

Table 1 Laboratory findings at first visit to our hospital

Hematology		Blood chemistry		Viral markers		Immunology		Coagulation	
WBC	7400/μL	TP	7.4 g/dL	Anti-HA IgM	(-)	IgA	183 mg/dL	PT%	95%
Neutrophil	72.0%	Albumin	4.5 g/dL	Anti-HCV	(-)	IgG	1168 mg/dL	APTT	36.4 s
Eosinophil	1.0%	T-Bil	11.1 mg/dL	HBsAg	(+) 197333	IgM	220 mg/dL		
Basophil	0.0%	D-Bil	8.0 mg/dL	Anti-HBc IgM	(+) 25.5 C.O.I	ANA	× 40, homogeneous		
Monocyte	10.0%	AST	1942 IU/L	HBeAg	(+) 253 C.O.I				
Lymphocyte	17.0%	ALT	2963 IU/L	Anti-HBe	(-) 0.0 %				
RBC	457/μL	ALP	612 IU/L	HBV-DNA	7.7 log copies/mL				
Hemoglobin	16.0 g/dL	γGTP	756 IU/L	Anti-HIV	(-)				
Hematocrit	46.4%	LDH	739 IU/L	RPR	(-)				
Platelet	36.6 × 10^4/μL	BUN	8.2 mg/dL	TPHA	(+)				
		Creatinine	0.64 mg/dL	Anti-CMV IgG	(+)				
		T-Chol	225 mg/dL	Anti-CMV IgM	(-)				
				Anti-EBV EBNA	(+)				
				Anti-EBV EA IgG	(-)				
				Anti-EBV VCA IgG	(+)				
				Anti-EBV VCA IgM	(-)				

WBC: White blood cells; RBC: Red blood cells; ANA: Antinuclear antibody; TP: Total protein; T-Bil: Total bilirubin; D-Bil: Direct bilirubin; AST: Aspartate aminotransferase; ALT: Alanine aminotransferase; ALP: Alkaline phosphatase; γGTP: γ-glutamyltranspeptidase; LDH: Lactase dehydrogenase; BUN: Blood urea nitrogen; T-Chol: Total cholesterol; PT: Prothrombin activity; APTT: Activated partial thromboplastin time; C.O.I: Cutoff index; HA: Hepatitis A; HCV: Hepatitis C virus; HBsAg: Hepatitis B surface antigen; HBc: Hepatitis B core; HBeAg: Hepatitis B e-antigen; HBV: Hepatitis B virus; HIV: Human immunodeficiency virus; RPR: Rapid plasma regain; TPHA: Treponema pallidum hemagglutination assay; CMV: Cytomegalovirus; EBV: Epstein-Barr virus; EBNA: Epstein-Barr virus nuclear antigen; EA: Early antigen; VCA: Viral capsid antigen.

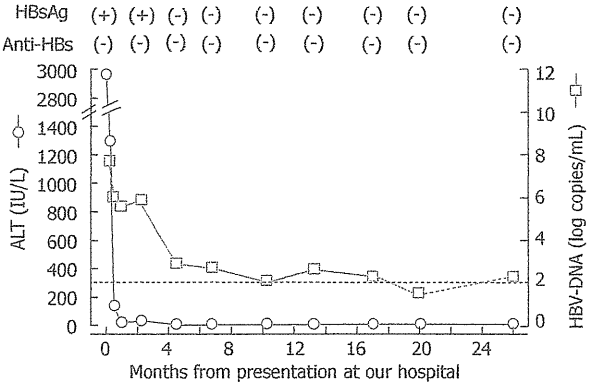

Figure 1 Clinical course of the patient infected with the genotype H strain. The dotted line indicates the detection limit of HBV-DNA (2.1 log copy/mL); the titer of the HBV-DNA was below the lower limit at 18 mo. HBsAg: Hepatitis B surface antigen; Anti-HBs: Antibody to hepatitis B surface antigen; ALT: Alanine aminotransferase; HBV: Hepatitis B virus.

(94 ℃, 30 s; 60 ℃, 30 s; 72 ℃, 30 s) with TAKARA LA Taq® DNA polymerase (TAKARA, Shiga, Japan). The amplified fragments were sequenced directly with an automated DNA sequencer (3500 Genetic Analyzer, Applied Biosystems, Foster City, CA, United States).

The genome of the infecting HBV (designated as B-MHJ9014) was 3215 bases in size. A phylogenetic analysis was performed with this strain and several database reference strains. B-MHJ9014 sorted with the genotype-H branch of the tree and clustered with the genotype-H strains previously isolated from Japanese patients (Figure 2). The substitutions at nt 1762 and nt 1764 (the basal core promoter region) and at nt 1896 (the precore region) were not observed. The length of the deduced amino acid sequences of the S, X, Core, and P proteins were identical to those encoded by other genotype H strains in the databases. The α determinant region of the S protein of B-MHJ9014 harbored an amino acid polymorphism (phenylalanine to leucine) at residue 134. The predicted B-MHJ9014 reverse transcriptase did not include any of the amino acid substitutions known to be associated with nucleotide analog resistance. To assess the complexity of the infecting virus, S region sequences from 51 clones in acute phase serum were determined. The detected sequences were genotype H and were closely related to the consensus sequence determine by direct sequencing with 1-3 amino acids polymorphisms (data not shown).

To assess the presence of human genome SNPs in the HLA-DP locus that are associated with persistent infection by HBV[14,15], a blood specimen was obtained from the patient (who had previously provided informed consent). Genomic DNA was extracted from buffy coat samples with the QIAamp DNA Mini kit (QIAGEN); DNA for SNPs rs3077 and rs9277535 were amplified with the appropriate primers and TAKARA LA Taq® DNA polymerase and were sequenced directly. The patient was homozygous (G/G) at both of these SNPs; these alleles are considered to be risk alleles for persistent infection.

DISCUSSION

HBV genotype H was first reported in 2002[5]. Infections by this genotype have been found mainly in Nicaragua, Mexico, and California; this genotype is considered to be rare in Asia, particularly in Japan[5,16-18]. However, since the first recognition of genotype H in Japan in 2005, eight strains have been isolated from Japanese patients (Table 2)[18-25]. All reported genotype H strains were isolated from male patients aged 35 to 65 years old, and the major route of infection was sexual transmission (5/8, 62.5%). Four cases (50%) represent transmissions that

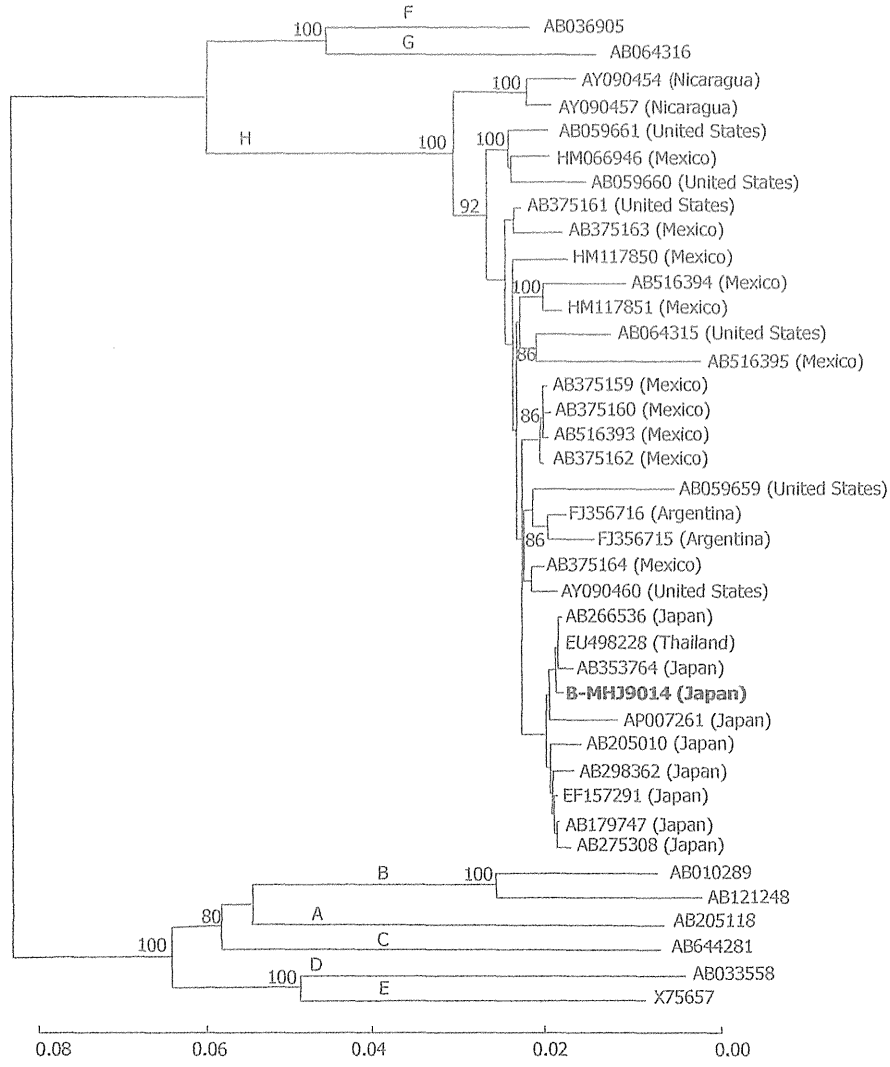

Figure 2 A phylogenetic trees constructed using the neighbor-joining method with the full hepatitis B virus genome sequence of the isolated and reference strains. The strain isolated in this case (B-MHJ9014) is shown in bold. The horizontal bar indicates the number of nucleotide substitutions per site. The reference sequences are shown with the DDBJ/EMBL/GenBank accession numbers. The HBV genotypes are indicated on each branch. The bootstrap values (> 80%) are indicated at the nodes as a percentage of the data obtained from 1000 resamplings. HBV: Hepatitis B virus.

Table 2 Genotype H strains reported in Japan

No.	Patient		Hypothesized source of infection		HIV infection[1]	Clinical feature	Accession number (Ref.)
	Age	Gender	Route	Place			
1	52	Male	Unknown	Japan	NA	Unknown blood donor	AB179747, [18]
2	61	Male	Sexual contact (heterosexual)	Thailand	NA	Chronic	AB205010, [19]
3	46	Male	Sexual contact (bisexual)	South America	(+)	Chronic	AP007261, [20]
4	38	Male	Sexual contact (homosexual)	Unknown	NA	Chronic	AB298362, [21]
5	65	Male	Unknown	Japan	NA	Acute	EF157291, [22]
6	35	Male	Unknown	Japan	NA	Acute	AB266536, [23]
7	60	Male	Sexual contact (homosexual)	Japan	(-)	Acute	AB275308, [24]
8	60	Male	Sexual contact (heterosexual)	Unknown	(+)	Chronic	AB353764, [25]
9	47	Male	Unknown	Japan	(-)	Acute to chronic	AB846650, this paper

[1]NA: Not available; HIV: Human immunodeficiency virus.

occurred in Japan. Co-infection with HIV was not common (2/8, 25%). These characteristics were similar to the case described here. All isolated strains from Japanese patients clustered together as a branch on the phylogenetic tree; therefore, it is possible that a specific strain of genotype H has emerged and spread in Japan. Presumably, the infrequent use of a reliable and convenient detection kit for genotype H infection has hampered the

correct diagnosis of genotype H infection; some cases may be misdiagnosed and considered to be infections by other genotypes. In fact, in the current case, our HBV isolate was originally identified as genotype C by the commercial kit that is covered by insurance in Japan. This kit was developed before the discovery of genotype H; thus, such a misidentification is a potential risk, as noted in the kit's instruction manual. The clinical features of genotype H infection remain obscure. There is a growing need for an accumulation of genotype H infection cases. To this end, the use of a reliable HBV genotyping kit that can correctly distinguish all genotypes is essential for routine clinical practice.

In Japan, most cases of acute hepatitis B are self-limiting, but some cases have been reported to have progressed to persistent infections[9,26-29]. Among the reported cases of genotype H infection, 4 strains were isolated from chronic hepatitis patients; in all cases, the infection was ascribed to sexual contact (Table 2)[19-21,25]. In our case, the HBV-DNA persisted for at least 26 mo. To our knowledge, this report represents the only case of genotype H infection in which chronic hepatitis was observed following acute infection. HBsAg was no longer detected at 4 mo from onset by HISCL-2000i. This disappearance was also confirmed by ARCHITECT® HBsAg (CMIA, Abbott Japan, Tokyo, Japan). In the S protein analysis, we found an amino acid polymorphism in the α determinant region. This polymorphism may affect the sensitivity for detecting HBsAg. HIV infection, a well-known risk factor for prolonged HBV infection[30], was not detected in our patient. Recently, the risk factors for HBV persistent infection have been reported in an analysis of a cohort that excluded patients co-infected with HIV[29]. In that report, infection with genotype A, elevated peak levels of HBV-DNA, and attenuated peak levels of ALT were suggested as risk factors for chronic infection. In the case described here, the peak level of HBV-DNA was 7.7 log copy/mL, which was consistent with increased risk for chronic infection. However, our patient exhibited a peak level of ALT of 2963 IU/L, which is a value that would classify this individual in the self-limiting group. Therefore, the clinical features of this case did not completely fit the risk factors associated with the establishment of chronic infection in the previous analysis[29]. Another reported risk factor for chronic HBV infection is the presence of certain SNP alleles. Specifically, selected SNPs around the HLA-DP locus have been reported to be associated with chronic hepatitis B in Asians[14,15]. With the informed consent of our patient, we determined the sequences for these SNPs (rs3077 and rs9277535) and found that this patient harbored risk alleles at both polymorphisms. This factor may have contributed to the establishment of chronic infection in this case.

In conclusion, we report a case of acute hepatitis B caused by a genotype H strain of HBV. This patient exhibited persistent infection. Our finding suggests that the infection of HBV genotype H can be a risk factor for persistent infection. We believe that it is necessary to use kits that are capable of accurate genotyping to permit an accumulation of cases and to investigate the clinical features of genotype H infection in routine clinical practice.

COMMENTS

Case characteristics

The main symptoms were nausea, loss of appetite, and a feeling of fullness in the abdomen.

Clinical diagnosis

The patient was a case of acute hepatitis B caused by a genotype H strain with persistent infection.

Differential diagnosis

The hepatitis B virus (HBV) genotype was considered to be important to predict the outcome and clinical features.

Laboratory diagnosis

To diagnose this patient, the detection of HBV markers and the complete determination of the HBV genotype were essential.

Treatment

The anti-viral treatment was not administered because we expected this case was self-limiting. Authors are now preparing medication.

Experiences and lessons

The infection of HBV genotype H can be a risk factor for persistent infection and the complete determination of HBV genotype is important.

Peer review

To conclude the association between HBV genotype H and chronic infection, the accumulation of cases of genotype H infection is essential.

REFERENCES

1 **World Health Organization**. Hepatitis B Fact Sheet. Accessed August 2013. Available from: URL: http://www.whoint/mediacentre/factsheets/fs204/en/indexhtml

2 **Okamoto H**, Tsuda F, Sakugawa H, Sastrosoewignjo RI, Imai M, Miyakawa Y, Mayumi M. Typing hepatitis B virus by homology in nucleotide sequence: comparison of surface antigen subtypes. *J Gen Virol* 1988; **69** (Pt 10): 2575-2583 [PMID: 3171552 DOI: 10.1099/0022-1317-69-10-2575]

3 **Norder H**, Courouce AM, Magnius LO. Complete genomes, phylogenetic relatedness, and structural proteins of six strains of the hepatitis B virus, four of which represent two new genotypes. *Virology* 1994; **198**: 489-503 [PMID: 8291231 DOI: 10.1006/viro.1994.1060]

4 **Stuyver L**, De Gendt S, Van Geyt C, Zoulim F, Fried M, Schinazi RF, Rossau R. A new genotype of hepatitis B virus: complete genome and phylogenetic relatedness. *J Gen Virol* 2000; **81**: 67-74 [PMID: 10640543]

5 **Arauz-Ruiz P**, Norder H, Robertson BH, Magnius LO. Genotype H: a new Amerindian genotype of hepatitis B virus revealed in Central America. *J Gen Virol* 2002; **2002**: 2059-2073

6 **Kurbanov F**, Tanaka Y, Mizokami M. Geographical and genetic diversity of the human hepatitis B virus. *Hepatol Res* 2010; **40**: 14-30 [PMID: 20156297 DOI: 10.1111/j.1872-034X.2009.00601.x]

7 **Kobayashi M**, Arase Y, Ikeda K, Tsubota A, Suzuki Y, Saitoh S, Kobayashi M, Suzuki F, Akuta N, Someya T, Matsuda M, Sato J, Kumada H. Clinical characteristics of patients infected with hepatitis B virus genotypes A, B, and C. *J Gastroenterol* 2002; **37**: 35-39 [PMID: 11824798]

8 **Tamada Y**, Yatsuhashi H, Masaki N, Nakamuta M, Mita E, Komatsu T, Watanabe Y, Muro T, Shimada M, Hijioka T, Satoh T, Mano Y, Komeda T, Takahashi M, Kohno H, Ota H, Hayashi S, Miyakawa Y, Abiru S, Ishibashi H. Hepatitis B virus strains of subgenotype A2 with an identical sequence spreading rapidly from the capital region to all over Japan in patients with acute hepatitis B. *Gut* 2012; **61**: 765-773 [PMID: 22068163 DOI: 10.1136/gutjnl-2011-300832]

9 **Yotsuyanagi H**, Ito K, Yamada N, Takahashi H, Okuse C, Yasuda K, Suzuki M, Moriya K, Mizokami M, Miyakawa Y,

Koike K. High levels of hepatitis B virus after the onset of disease lead to chronic infection in patients with acute hepatitis B. *Clin Infect Dis* 2013; 57: 935-942 [PMID: 23704123 DOI: 10.1093/cid/cit348]
10 **Kao JH**, Chen PJ, Lai MY, Chen DS. Hepatitis B genotypes correlate with clinical outcomes in patients with chronic hepatitis B. *Gastroenterology* 2000; 118: 554-559 [PMID: 10702206]
11 **Orito E**, Mizokami M, Sakugawa H, Michitaka K, Ishikawa K, Ichida T, Okanoue T, Yotsuyanagi H, Iino S. A case-control study for clinical and molecular biological differences between hepatitis B viruses of genotypes B and C. Japan HBV Genotype Research Group. *Hepatology* 2001; 33: 218-223 [PMID: 11124839 DOI: 10.1053/jhep.2001.20532]
12 **Chu CJ**, Lok AS. Clinical significance of hepatitis B virus genotypes. *Hepatology* 2002; 35: 1274-1276 [PMID: 11981779 DOI: 10.1053/jhep.2002.33161]
13 **Miyakawa Y**, Mizokami M. Classifying hepatitis B virus genotypes. *Intervirology* 2003; 46: 329-338 [PMID: 14688448]
14 **Kamatani Y**, Wattanapokayakit S, Ochi H, Kawaguchi T, Takahashi A, Hosono N, Kubo M, Tsunoda T, Kamatani N, Kumada H, Puseenam A, Sura T, Daigo Y, Chayama K, Chantratita W, Nakamura Y, Matsuda K. A genome-wide association study identifies variants in the HLA-DP locus associated with chronic hepatitis B in Asians. *Nat Genet* 2009; 41: 591-595 [PMID: 19349983 DOI: 10.1038/ng.348]
15 **Nishida N**, Sawai H, Matsuura K, Sugiyama M, Ahn SH, Park JY, Hige S, Kang JH, Suzuki K, Kurosaki M, Asahina Y, Mochida S, Watanabe M, Tanaka E, Honda M, Kaneko S, Orito E, Itoh Y, Mita E, Tamori A, Murawaki Y, Hiasa Y, Sakaida I, Korenaga M, Hino K, Ide T, Kawashima M, Mawatari Y, Sageshima M, Ogasawara Y, Koike A, Izumi N, Han KH, Tanaka Y, Tokunaga K, Mizokami M. Genome-wide association study confirming association of HLA-DP with protection against chronic hepatitis B and viral clearance in Japanese and Korean. *PLoS One* 2012; 7: e39175 [PMID: 22737229 DOI: 10.1371/journal.pone.0039175]
16 **Flichman D**, Galdame O, Livellara B, Viaut M, Gadano A, Campos R. Full-length genome characterization of hepatitis B virus genotype H strain isolated from serum samples collected from two chronically infected patients in Argentina. *J Clin Microbiol* 2009; 47: 4191-4193 [PMID: 19794035 DOI: 10.1128/jcm.01337-09]
17 **Roman S**, Tanaka Y, Khan A, Kurbanov F, Kato H, Mizokami M, Panduro A. Occult hepatitis B in the genotype H-infected Nahuas and Huichol native Mexican population. *J Med Virol* 2010; 82: 1527-1536 [PMID: 20648606 DOI: 10.1002/jmv.21846]
18 **Ohnuma H**, Yoshikawa A, Mizoguchi H, Okamoto H. Characterization of genotype H hepatitis B virus strain identified for the first time from a Japanese blood donor by nucleic acid amplification test. *J Gen Virol* 2005; 86: 595-599 [PMID: 15722519 DOI: 10.1099/vir.0.80732-0]
19 **Nakajima A**, Usui M, Huy TT, Hlaing NK, Masaki N, Sata T, Abe K. Full-length sequence of hepatitis B virus belonging to genotype H identified in a Japanese patient with chronic hepatitis. *Jpn J Infect Dis* 2005; 58: 244-246 [PMID: 16116261]
20 **Shibayama T**, Masuda G, Ajisawa A, Hiruma K, Tsuda F, Nishizawa T, Takahashi M, Okamoto H. Characterization of seven genotypes (A to E, G and H) of hepatitis B virus recovered from Japanese patients infected with human immunodeficiency virus type 1. *J Med Virol* 2005; 76: 24-32 [PMID: 15779062 DOI: 10.1002/jmv.20319]
21 **Suzuki F**, Akuta N, Suzuki Y, Yatsuji H, Sezaki H, Arase Y, Kawamura Y, Hosaka T, Kobayashi M, Ikeda K, Kobayashi M, Watahiki S, Kumada H. Selection of a virus strain resistant to entecavir in a nucleoside-naive patient with hepatitis B of genotype H. *J Clin Virol* 2007; 39: 149-152 [PMID: 17442615 DOI: 10.1016/j.jcv.2007.03.004]
22 **Tamada Y**, Yano K, Komatsu T, Yatsuhashi H, Ishibashi H, Takahashi K, Mishiro S. First Domestic Case of Acute Hepatitis Caused by an HBV genotype H Strain. *Kanzo* 2007; 48: 109-111 [DOI: 10.2957/kanzo.48.109]
23 **Kumagai I**, Abe K, Oikawa T, Sato A, Sato S, Endo R, Takikawa Y, Suzuki K, Masuda T, Sainokami S, Endo K, Takahashi M, Okamoto H. A male patient with severe acute hepatitis who was domestically infected with a genotype H hepatitis B virus in Iwate, Japan. *J Gastroenterol* 2007; 42: 168-175 [PMID: 17351807 DOI: 10.1007/s00535-006-1963-2]
24 **Chihara N**, Arase Y, Suzuki F, Suzuki Y, Kobayashi M, Akuta N, Hosaka T, Sezaki H, Yatsuji H, Kawamura Y, Kobayashi M, Watahiki S, Ikeda K, Kumada H. Prolonged hepatitis after acute infection with genotype H hepatitis B virus. *Intern Med* 2007; 46: 1847-1851 [PMID: 18025766]
25 **Kanada A**, Takehara T, Ohkawa K, Kato M, Tatsumi T, Miyagi T, Sakamori R, Yamaguchi S, Uemura A, Kohga K, Sasakawa A, Hikita H, Kawamura K, Kanto T, Hiramatsu N, Hayashi N. Early emergence of entecavir-resistant hepatitis B virus in a patient with hepatitis B virus/human immunodeficiency virus coinfection. *Hepatol Res* 2008; 38: 622-628 [PMID: 18070052 DOI: 10.1111/j.1872-034X.2007.00307.x]
26 **Suzuki Y**, Kobayashi M, Ikeda K, Suzuki F, Arfase Y, Akuta N, Hosaka T, Saitoh S, Kobayashi M, Someya T, Matsuda M, Sato J, Watabiki S, Miyakawa Y, Kumada H. Persistence of acute infection with hepatitis B virus genotype A and treatment in Japan. *J Med Virol* 2005; 76: 33-39 [PMID: 15779048 DOI: 10.1002/jmv.20320]
27 **Ozasa A**, Tanaka Y, Orito E, Sugiyama M, Kang JH, Hige S, Kuramitsu T, Suzuki K, Tanaka E, Okada S, Tokita H, Asahina Y, Inoue K, Kakumu S, Okanoue T, Murawaki Y, Hino K, Onji M, Yatsuhashi H, Sakugawa H, Miyakawa Y, Ueda R, Mizokami M. Influence of genotypes and precore mutations on fulminant or chronic outcome of acute hepatitis B virus infection. *Hepatology* 2006; 44: 326-334 [PMID: 16871568 DOI: 10.1002/hep.21249]
28 **Miyoshi T**, Hiraoka A, Hidaka S, Shimizu Y, Ninomiya K, Utsunomiya H, Tazuya N, Tanihira T, Hasebe A, Miyamoto Y, Ninomiya T, Abe M, Hiasa Y, Onji M, Michitaka K. An adult patient with acute infection with hepatitis B virus genotype C that progressed to chronic infection. *Intern Med* 2012; 51: 173-176 [PMID: 22246485]
29 **Ito K**, Yotsuyanagi H, Yatsuhashi H, Karino Y, Takikawa Y, Saito T, Arase Y, Imazeki F, Kurosaki M, Umemura T, Ichida T, Toyoda H, Yoneda M, Mita E, Yamamoto K, Michitaka K, Maeshiro T, Tanuma J, Tanaka Y, Sugiyama M, Murata K, Masaki N, Mizokami M. Risk factors for long-term persistence of serum hepatitis B surface antigen following acute hepatitis B virus infection in Japanese adults. *Hepatology* 2014; 59: 89-97 [PMID: 23897861 DOI: 10.1002/hep.26635]
30 **Gilson RJ**, Hawkins AE, Beecham MR, Ross E, Waite J, Briggs M, McNally T, Kelly GE, Tedder RS, Weller IV. Interactions between HIV and hepatitis B virus in homosexual men: effects on the natural history of infection. *AIDS* 1997; 11: 597-606 [PMID: 9108941]

P- Reviewers: Chan KM, Chun YH, Rodriguez-Frias F
S- Editor: Qi Y **L- Editor**: A **E- Editor**: Wu HL

Hepatology Research

Hepatology Research 2014; 44: 1047–1055 doi: 10.1111/hepr.12221

Original Article

Discrimination of fibrotic staging of chronic hepatitis C using multiple fibrotic markers

Kenji Ikeda,[1,2] Namiki Izumi,[3] Eiji Tanaka,[8] Hiroshi Yotsuyanagi,[4] Yoshihisa Takahashi,[6] Junichi Fukushima,[7] Fukuo Kondo,[6] Toshio Fukusato,[6] Kazuhiko Koike,[5] Norio Hayashi,[9] Hirohito Tsubouchi[10] and Hiromitsu Kumada[1,2]

[1]*Department of Hepatology, Toranomon Hospital,* [2]*Okinaka Memorial Institute for Medical Research,* [3]*Department of Gastroenterology, Musashino Red Cross Hospital,* [4]*Department of Infectious Disease,* [5]*Department of Gastroenterology, Graduate School of Medicine, Tokyo University,* [6]*Department of Pathology, Teikyo University School of Medicine,* [7]*Department of Pathology, NTT Medical Center Tokyo, Tokyo,* [8]*Department of Gastroenterology, Shinshu University of Medicine, Matsumoto,* [9]*Department of Gastroenterology, Kansai-Rosai Hospital, Hyogo, and* [10]*Department of Gastroenterology, Kagoshima University of Medicine, Kagoshima, Japan*

Aim: In order to evaluate and judge a fibrotic stage of patients with chronic hepatitis C, multivariate regression analysis was performed using multiple fibrotic markers.

Methods: A total of 581 patients from eight hepatology units and institutes were diagnosed by needle biopsy as having chronic liver disease caused by hepatitis C virus. Twenty-three variables and their natural logarithmic transformation were employed in the multivariate analysis.

Results: Multivariate regression analysis finally obtained the following function: $z = 2.89 \times ln$ (type IV collagen 7S) (ng/mL) $- 0.011 \times$ (platelet count) ($\times 10^3/mm^3$) $+ 0.79 \times ln$ (total bilirubin) (mg/dL) $+ 0.39 \times ln$ (hyaluronic acid) (μg/L) $- 1.87$. Median values of the fibrotic score of F1 ($n = 172$), F2 ($n = 80$), F3 ($n = 37$) and F4 ($n = 16$) were calculated as 1.00, 1.45, 2.82 and 3.83, respectively. Multiple regression coefficient and coefficient of determination were 0.56 and 0.320, respectively. Validation with patient data from other institutions demonstrated good reproducibility of the fibrotic score for hepatitis C (FSC), showing 1.10 in F1 ($n = 156$), 2.35 in F2 ($n = 73$), 3.16 in F3 ($n = 36$) and 3.58 in F4 ($n = 11$).

Conclusion: A concise multiple regression function using four laboratory parameters successfully predicted pathological fibrotic stage of patients with hepatitis C virus infection.

Key words: chronic hepatitis, hepatitis C virus, liver cirrhosis, liver fibrosis, multiple regression analysis, stage

INTRODUCTION

WHEN HEPATITIS C virus (HCV)-related chronic liver disease was found by biochemical and virological examination, peritoneoscopy and/or liver biopsy can establish the definitive diagnosis of chronic hepatitis and liver cirrhosis. Although these pathological procedures are reliable and informative both in diagnosis and treatment, they sometimes require medical invasion and financial costs, including the risk of bleeding from needle puncture, some pain experienced during the examination, medical expenses and hospitalization for a few days. The pathological examination is, therefore, rarely performed repeatedly in a short period of time, even when disease activity is severe and progression of liver disease is highly suspected. Recently, many authors described the usefulness of ultrasonographic elastography and magnetic resonance imaging technology in the estimation of staging of chronic hepatitis and cirrhosis.[1–4] These ways of estimation using the imaging apparatuses seem truly useful for current patients, but it cannot evaluate and compare with past fibrotic states of patients retrospectively. Moreover, the same apparatus for elastometry will not be available for repeated measurement for a follow-up examination, several years later for example.

In spite of the accuracy of biopsy and of convenience of elastography in chronic liver disease, clinical diagnosis based on biochemistry and hematology is still indispensable for the daily practice of many patients with

Correspondence: Dr Kenji Ikeda, *Department of Hepatology, Toranomon Hospital, 2-2-2 Toranomon, Minato-ku, Tokyo 105-8470, Japan. Email: ikedakenji@tora.email.ne.jp*

Received 13 May 2013; revision 4 August 2013; accepted 8 August 2013.

HCV-related liver disease. Recently, several studies were published about estimation of hepatitis stages, using one or more serum biomarkers. Discriminant functions or multivariate analyses demonstrated that approximately 60–90% of patients with chronic hepatitis C were correctly classified as mild hepatitis and severe hepatitis with advanced fibrosis.[5–16] The usefulness of the discriminant functions was, however, less valuable up to the present time for a few reasons. First, these functions were made for the purpose of discrimination of severe hepatic fibrosis from mild fibrosis, and four histological classifications (F1, F2, F3 and F4) were selected in almost of the studies. Second, some studies analyzed both hepatitis B virus and HCV infection, although the significance and actual values of each liver function test in the evaluation of the severity of liver disease were not similar among each viral hepatitis and alcoholic liver disease. Third, biochemical markers for liver fibrosis (e.g. hyaluronic acid, type IV collagen, procollagen III peptide)[17–19] were not always included in those previous studies.

We tried to generate a function estimating fibrotic stages of HCV-related chronic hepatitis, which were objectively diagnosed by liver biopsy. The purpose of this study is, therefore, to make a reliable multiple regression function and to obtain practical coefficients for significant variables also using fibrotic markers.

METHODS

Patients

A TOTAL OF 605 Japanese patients with chronic hepatitis C were recruited for the study from eight hospitals in Japan: Toranomon Hospital, Hiroshima University Hospital (K. Chayama, M.D.), Ehime University Hospital (M. Onji, M.D.), Musashino Red Cross Hospital (N. Izumi, M.D.), Shishu University Hospital (E. Tanaka, M.D.), Showa University Hospital (M. Imawari, M.D.), Osaka University Hospital (T. Takehara, M.D.) and Kagoshima University Hospital (H. Tsubouchi, M.D.). Inclusion criteria for this study were: (i) positive HCV antibody for more than 6 months; (ii) persistent or intermittent elevation in aspartate aminotransferase (AST)/alanine aminotransferase (ALT) levels; and (iii) liver biopsy showing chronic hepatitis (F1, F2, F3 or F4). We excluded those patients with overt alcoholic liver disease or fatty liver, association of other types of liver disease (e.g. hepatitis B, primary biliary cirrhosis, autoimmune hepatitis), or those associated with hepatocellular carcinoma or other malignancy. Among the patients, 603 fulfilled the conditions for the study: complete demographic data, basic laboratory data of hematology and biochemistry, required liver biopsy specimens, and sufficient amount of frozen sera. We also excluded an additional 22 patients with eventual histological diagnosis of F0 stage.

Finally, a total of 581 patients who were diagnosed as having chronic hepatitis or cirrhosis (F1, F2, F3 or F4) were analyzed for the following hematological, biochemical and histopathological examination. There were 305 males and 276 females aged 15–78 with a median of 55 years.

All the patients presented written informed consent in individual hospitals and medical centers, and the study was approved by each ethical committee.

Hematological and biochemical examination

Hematological and standard biochemical evaluation had been performed in each medical institution: white blood cell, red blood cell count, hemoglobin, platelet count, total bilirubin, AST, ALT, AST/ALT ratio (AAR), γ-glutamyltransferase (GGT), total protein, albumin and γ-globulin.

Special biochemical examinations including fibrotic markers were carried out using stored frozen sera at −20°C or lower: α2-macroglobulin, haptoglobin concentration, haptoglobin typing, apolipoprotein A1, hyaluronic acid, tissue inhibitor of matrix metalloproteinase (TIMP)-1, TIMP-2, procollagen III peptide and type IV collagen 7S.

Histological diagnosis of chronic hepatitis and cirrhosis

All of the 581 cases fulfilled required standards of histological evaluation: sufficient length of specimen, hematoxylin–eosin staining and at least one specimen with fiber staining. Four independent pathologists (Y. T., J. F., F. K. and T. F.), who were not informed of patients' background and laboratory features except for age and sex, evaluated the 581 specimens regarding the stages of fibrosis and activity. Pathological classification of chronic hepatitis staging was based on Desmet *et al.*[20]

Before judgment of histological staging of individual specimens, the pathologists discussed objective and reproducible judgment of pathological diagnosis of hepatitis. They made a panel for obvious criteria using typical microscopic pictures for each stage, and it was always referred to during the procedure of pathological judgment. When inconsistent results were found in the diagnosis of stage of hepatitis among the pathologists, the final judgment was accepted as the majority rule among them.

Statistical analysis

Non-parametric procedures were employed for the analysis of background characteristics and laboratory data among patients in each stage, including Mann–Whitney *U*-test, Kruskal–Wallis test and χ^2-test.

The normality of the distribution of the data was evaluated by Kolmogorov–Smirnov one-sample test. Because certain variables partly did not conform to a normal distribution, natural logarithmic transformation of bilirubin, AST, ALT, GGT, α2-macroglobulin, hyaluronic acid, type IV collagen 7S and TIMP-2 were also analyzed in the following calculation. The natural logarithmic transformation of the results yielded a normal distribution or symmetrical distribution for all the analyzed factors. After the procedures, the following multiple regression analysis became rationally robust against deviations from normal distribution. In order to avoid introducing into the model any variables that were mutually correlated, we checked the interaction between all pairs of the variables by calculating variance of inflation factors. Of the highly correlated variables, less significant factors were removed from the viewpoint of multicollinearity.

Multivariate regression analysis was performed using 305 patient data from Toranomon Hospital (training dataset), to generate training data of predicting function. We used a stepwise method for selection of informative subsets of explanatory variables in the model. Multiple regression coefficient and coefficient of determination are also taken into account in the selection of variables. Next, we validated the obtained predictive function using the remaining 276 patient data from the other seven liver institutions (validation dataset).

A *P*-value of less than 0.05 with two-tailed test was considered to be significant. Data analysis was performed using the computer program SPSS version 19.[21]

For evaluation of the efficiency and usefulness of obtained function for estimation of fibrosis, we compared various fibrotic scores for hepatitis C, including AAR,[8] AST-to-platelet ratio index (APRI),[12] FIB-4[13] and FibroTest.[9]

RESULTS

Pathological diagnosis

FOUR PATHOLOGISTS INDEPENDENTLY judged the fibrotic stages and inflammatory activity for 581 specimens of chronic hepatitis/cirrhosis caused by HCV. A total of 328 patients (56.5%) had a fibrotic stage of F1, 153 (26.3%) F2, 73 (12.6%) F3 and 27 (4.6%) F4. In the training subgroup ($n = 305$), judgment of F1 was made in 172, F2 in 80, F3 in 37 and F4 in 16. In the validation group ($n = 276$), judgment as F1 was made in 156, F2 in 73, F3 in 36 and F4 in 11.

According to hepatitis activity classification, A0 was found in nine patients (1.52%), A1 in 350 (60.2%), A2 in 198 (34.1%) and A3 in 24 (4.1%).

Laboratory data of each hepatitis stage in training group

There were 161 males and 144 females with a median age of 54 years (range, 22–69). Laboratory data of the 305 patients in the training group are shown in Table 1. Although several individual items were well correlated with the severity of hepatic fibrosis, significant overlap values were noted among F1 to F4 stages: platelet count, GGT, γ-globulin, hyaluronic acid and type IV collagen 7S.

Regression function generated from training patient group

After stepwise variable selection, multivariate regression analysis finally obtained the following function: $z = 2.89 \times ln$ (type IV collagen 7S) (ng/mL) $- 0.011 \times$ (platelet count) ($\times 10^3$/mm^3) $+ 0.79 \times ln$ (total bilirubin) (ng/mL) $+ 0.39 \times ln$ (hyaluronic acid) (μm/L) $-$ 1.87. Median values of the fibrotic score of F1 ($n = 172$), F2 ($n = 80$), F3 ($n = 37$) and F4 stages ($n = 16$) were calculated as 1.00, 1.45, 2.82 and 3.83, respectively (Fig. 1). The multiple regression coefficient and coefficient of determination were 0.56 and 0.32, respectively.

A 55-year-old man with F1 fibrotic stage (Fig. 2a) showed serum type IV collagen concentration as 3.8 ng/mL, platelet as 152×10^3 count/mm^3, total bilirubin as 0.8 mg/dL and hyaluronic acid as 16 μg/L. The regression function provided his fibrotic score as 1.16. Another man aged 43 years had F3 fibrosis with severe hepatitis activity of A3 on histological examination (Fig. 2b). His type IV collagen was 11.0 ng/mL, platelet 162×10^3 count/mm^3, total bilirubin 0.7 mg/dL and hyaluronic acid 189 μg/L, and regression function calculated his fibrotic score as 4.98.

Validation of discriminant function

Validation data of 276 patients (Table 2) were collected from the other seven institutions in Japan. When applying the regression function for the validation set, the fibrotic score for hepatitis C (FSC) demonstrated good reproducibility, showing 1.10 in patients with chronic hepatitis of F1 ($n = 156$), 2.35 in F2 ($n = 73$), 3.16 in F3 ($n = 36$) and 3.58 in F4 ($n = 11$) (Fig. 3). Although F4

Table 1 Demography and laboratory data of 305 patients in training group

	F1 ($n = 172$)	F2 ($n = 80$)	F3 ($n = 37$)	F4 ($n = 16$)
Demography				
Males : females	97:75	38:42	20:17	6:10
Age (median, range)	51 (22–69)	55 (29–68)	55 (27–69)	56.5 (29–65)
Laboratory data (median, range)				
WBC ($\times 10^3/mm^3$)	4.7 (2.0–10.1)	4.3 (2.3–8.5)	4.5 (2.9–6.8)	4.7 (3.3–6.9)
Hemoglobin(g/dL)	14.6 (11.0–18.2)	14.4 (9.3–17.4)	14.6 (11.5–17.7)	14.55 (12.1–16.5)
Platelet ($\times 10^3/mm^3$)	183 (52–364)	161 (82–387)	131 (74–237)	124 (7.7–191)
Albumin (g/dL)	4.1 (2.3–4.9)	4.0 (3.5–4.6)	3.9 (3.1–4.6)	3.8 (3.3–4.3)
Bilirubin (mg/dL)	0.8 (0.2–1.9)	0.7 (0.3–1.7)	0.9 (0.4–7.5)	0.8 (0.5–7.4)
AST (IU/L)	42 (16–386)	61 (16–332)	63 (13–238)	71 (30–160)
ALT (IU/L)	60.5 (12–1664)	84.5 (10–647)	108 (27–415)	90.5 (36–264)
γ-GTP (IU/L)	40 (7–383)	48 (10–262)	54 (13–209)	58 (21–195)
γ-Globulin (g/dL)	1.47 (0.58–3.40)	1.61 (1.02–2.41)	1.69 (0.66–2.64)	1.79 (1.22–2.73)
γ-Globulin (%)	19.4 (10.0–40.5)	20.9 (14.0–28.3)	21.3 (8.1–30.4)	22.7 (16.5–36.9)
α2-Macroglobulin (mg/dL)	269 (123–505)	335 (154–551)	369 (183–627)	317 (207–511)
Haptoglobin (mg/dL)	94.5 (<5–265)	75.5 (<5–263)	56 (<5–2031)	75 (30–142)
Apolipoprotein A1 (mg/dL)	132 (71–209)	131 (73–207)	124 (98–166)	121 (83–153)
Hyaluronic acid (μg/L)	25 (<5–407)	41.5 (<5–263)	71 (<5–326)	89.5 (5–246)
TIMP-1 (ng/mL)	165 (73–291)	173 (97–302)	182 (126–308)	192.5 (128–260)
TIMP-2 (ng/mL)	77.5 (31–210)	80 (34–307)	76 (46–143)	78 (58–110)
Procollagen III peptide (U/mL)	0.75 (0.47–1.50)	0.805 (0.61–1.70)	0.86 (0.53–1.50)	1.05 (0.66–1.60)
Type IV collagen 7S (ng/mL)	4.0 (1.7–73)	4.3 (2.1–11.0)	5.2 (3.2–11.0)	5.8 (4.3–9.4)

γ-GTP, γ-glutamyl transpeptidase; ALT, alanine aminotransferase; AST, aspartate aminotransferase; TIMP, tissue inhibitor of matrix metalloproteinase; WBC, white blood cell.

fibrotic stage consisted of only 11 patients and the score 3.58 was regarded as a rather low value, the scores of other stages of fibrosis were concordant with histological fibrosis.

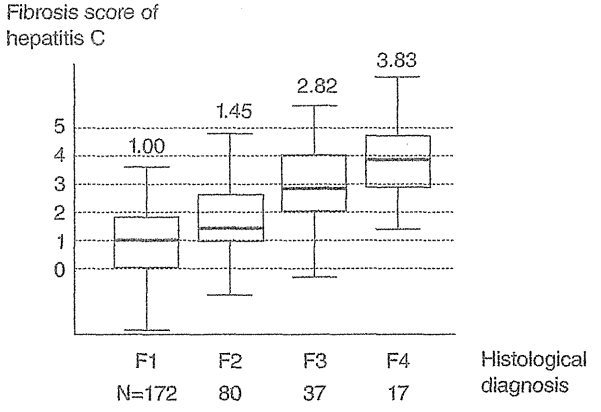

Figure 1 Box and whisker plots of fibrotic score of each group of histological fibrosis in the training dataset. Fibrotic score of hepatitis C (FSC) was generated by the function, $z = 2.89 \times ln$ (type IV collagen 7S) (ng/mL) $- 0.011 \times$ (platelet count) ($\times 10^3/mm^3$) $+ 0.79 \times ln$ (total bilirubin) (mg/dL) $+ 0.39 \times ln$ (hyaluronic acid) (μg/L) $- 1.87$.

Comparisons of efficacy with various fibrotic scores (Fig. 4)

In order to evaluate the efficacy and usefulness of the obtained FSC, we compared with previously reported fibrotic scores using training data. AAR, APRI, FIB-4 and FibroTest showed only slight correlation with actual histological stage. APRI and FIB-4 demonstrated increasing trends of the score associated with histological fibrosis, but significant overlapping scores were found through F1 to F4. Spearman's correlation coefficients of AAR, APRI, FIB-4 and FibroTest were 0.021 ($P = 0.707$), 0.462 ($P < 0.001$), 0.440 ($P < 0.001$) and 0.415 ($P < 0.001$), respectively. Our FSC showed Spearman's correlation coefficient of 0.572 ($P < 0.001$), and was of much higher value than the others.

DISCUSSION

RECOGNITION OF SEVERITY of chronic hepatitis is essential in managing patients with chronic HCV infection: estimation of length of infection, existence of any previous hepatitis activity, presumption of current fibrotic stage, and prediction of future fibrotic progression and hepatocarcinogenesis. Differential diagnosis of cirrhosis from chronic hepatitis is especially important

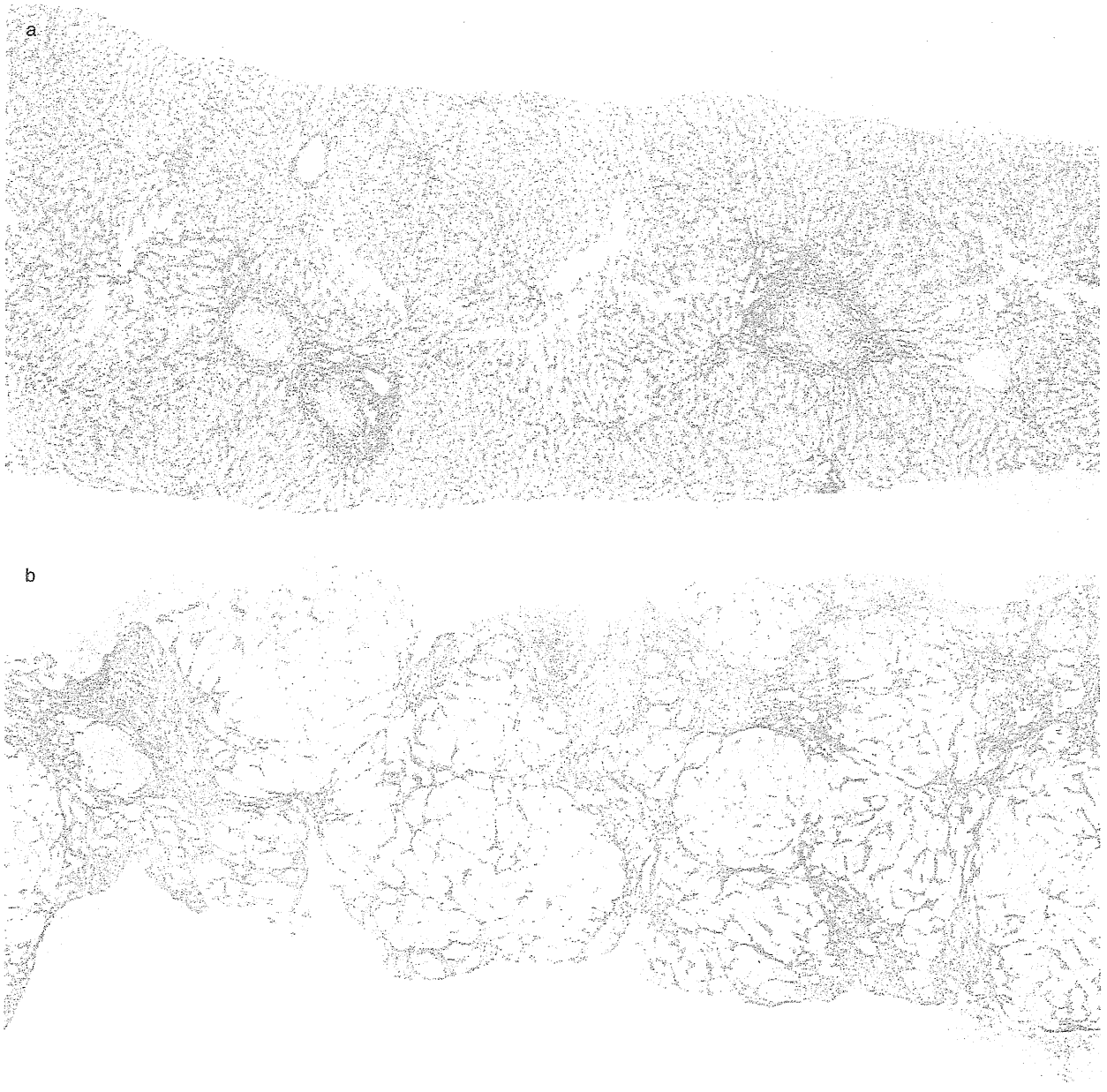

Figure 2 Case presentations of the training set. (a) A 55-year-old man with F1 fibrosis. Final regression function provided his fibrotic score as 1.16. (b) A 43-year-old man with F3 fibrosis with severe hepatitis activity. His regression coefficient was calculated as 4.98 (silver stain, ×40).

in the evaluation of chronic HCV infection. Identification of liver cirrhosis often leads to an important change in management of the patients: needs for fiberscopic examination for esophageal varices, ultrasonographic exploration for the association of liver cancer, and prediction of hepatic decompensation.

Recently, non-invasive estimation of severity of liver fibrosis has been reported in patients with HCV-related chronic hepatitis.[6–14] However, these studies were principally aimed at differentiation of advanced fibrotic stages of F3 or F4 from mild fibrotic stages of F1 or F2. Those discriminative functions were insufficient to

Table 2 Demography and laboratory data of 276 patients in validation group

	F1 ($n = 156$)	F2 ($n = 73$)	F3 ($n = 36$)	F4 ($n = 11$)
Demography				
Males : females	83:73	42:31	13:23	6:5
Age (median, range)	55 (15–74)	58 (32–77)	62.5 (30–78)	51 (38–73)
Laboratory data (median, range)				
WBC ($\times 10^3/mm^3$)	5.1 (2.1–10.5)	4.8 (2.6–9.0)	4.85 (2.3–14.2)	3.9 (3.2–6.0)
Hemoglobin (g/dL)	14.2 (8.9–17.7)	14.4 (11.8–17.4)	14.1 (10.1–16.4)	13.6 (8.9–16.3)
Platelet ($\times 10^3/mm^3$)	183 (59–440)	153 (80–265)	136 (64–348)	135 (79–153)
Albumin (g/dL)	4.3 (3.1–5.3)	4.3 (3.3–5.2)	4.05 (3.0–5.5)	3.9 (3.0–4.7)
Bilirubin (mg/dL)	0.7 (0.2–8.7)	0.7 (0.2–1.7)	0.8 (0.2–2.5)	0.8 (0.4–11.0)
AST (IU/L)	35 (11–1390)	49 (19–183)	80 (20–190)	96 (29–257)
ALT (IU/L)	49 (11–1635)	62 (12–575)	84 (14–218)	115 (29–303)
γ-GTP (IU/L)	35 (11–600)	52 (10–497)	51 (14–236)	112 (17–312)
γ-Globulin (g/dL)	1.47 (0.70–2.14)	1.60 (0.80–2.37)	1.71 (0.63–2.62)	2.19 (1.70–2.82)
γ-Globulin (%)	19.5 (9.2–26.4)	20.8 (10.8–30.8)	22.4 (9.5–29.9)	27.4 (21.8–35.3)
α2-Macroglobulin (mg/dL)	271.5 (126–572)	381 (172–573)	405.5 (196–594)	468 (242–655)
Haptoglobin (mg/dL)	95 (<5–305)	80 (<5–223)	63.5 (<5–192)	65 (<5–130)
Apolipoprotein A1 (mg/dL)	126 (45–198)	127 (63–191)	116 (46–172)	108 (62–171)
Hyaluronic acid (μg/L)	37.5 (<5–1260)	68 (5–1000)	140.5 (23–2610)	159 (33–364)
TIMP-1 (ng/mL)	157.5 (77–301)	172 (89–355)	188.5 (99–430)	192 (112–320)
TIMP-2 (ng/mL)	70 (21–294)	73 (21–207)	89 (27–280)	76 (36–120)
Procollagen III peptide (U/mL)	0.73 (0.52–8.30)	0.81 (0.53–1.60)	1.00 (0.63–1.90)	1.00 (0.68–1.60)
Type IV collagen 7S (ng/mL)	3.9 (1.2–12.0)	4.5 (2.3–9.9)	5.8 (2.8–16.0)	6.1 (4.6–10.0)

γ-GTP, γ-glutamyl transpeptidase; ALT, alanine aminotransferase; AST, aspartate aminotransferase; TIMP, tissue inhibitor of matrix metalloproteinase; WBC, white blood cell.

recognize the stepwise progression of viral hepatitis from F1 through F4. This dichotomy (mild or severe) of chronic hepatitis C seemed less valuable in the study of disease progression, disease control abilities of antiviral drugs and estimation of histological improvement after anti-inflammatory drugs. A histology-oriented, practical and reliable formula is therefore required for the diagnosis and investigation of chronic hepatitis C.

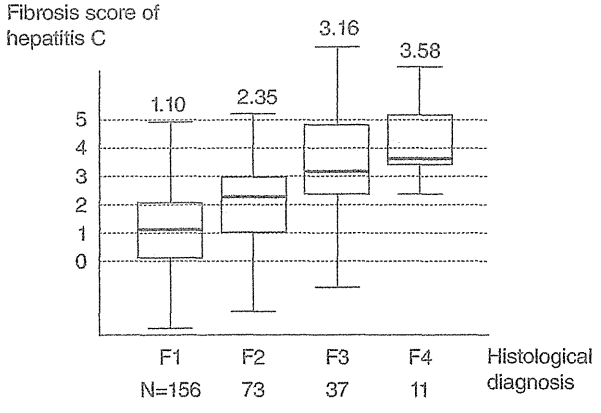

Figure 3 Box and whisker plots of fibrotic score of each group of histological fibrosis in the validation dataset. Fibrotic score of hepatitis C (FSC) was generated by the function, $z = 2.89 \times ln$ (type IV collagen 7S) (ng/mL) $- 0.011 \times$ (platelet count) ($\times 10^3/mm^3$) $+ 0.79 \times ln$ (total bilirubin) (ng/mL) $+ 0.39 \times ln$ (hyaluronic acid) (μg/L) $- 1.87$.

This study was aimed to establish non-invasive evaluation and calculation of liver fibrosis for patients with chronic HCV infection. Although it was retrospectively performed as a multicenter study of eight institutions, judgment of histological diagnosis was independently performed by four pathologists in the other hospital, informed of nothing except for the patient's age, sex and positive HCV infection. Objective judgment of the histological staging and grading in sufficient biopsy specimens could be obtained.

As many as 581 patients with chronic hepatitis C were analyzed in this study, who had been diagnosed as having chronic hepatitis or cirrhosis by liver biopsy performed in experienced liver units in Japan. To obtain the most suitable equation approximating histological fibrotic stage, multivariate analysis was performed using two demographic parameters (age and sex) and 21 hematological and biochemical markers with or without logarithmic transformation. They included many kinds of fibrotic markers: α2-macroglobulin, haptoglobin concentration, haptoglobin typing, apolipo-